Journal of Cleaner Production 414 (2023) 137561

Contents lists available at ScienceDirect

Journal of Cleaner Production

journal homepage: www.elsevier.com/locate/jclepro

Review

Phosphogypsum circular economy considerations: A critical review from more than 65 storage sites worldwide

Essaid Bilal [a], Hajar Bellefqih [a], Véronique Bourgier [a], Hamid Mazouz [b], Delia-Georgeta Dumitraş [c], Frédéric Bard [a], Marie Laborde [a,d], Jean Pierre Caspar [e], Bernard Guilhot [a], Elena-Luisa Iatan [a,f], Moussa Bounakhla [g], Măruţa Aurora Iancu [c], Ştefan Marincea [c], Meriem Essakhraoui [h], Binlin Li [i], Reymar R. Diwa [j], Jennyvi D. Ramirez [j], Yelizaveta Chernysh [k,l,m], Viktoriia Chubur [l], Hynek Roubík [l], Horst Schmidt [n], Redouane Beniazza [o], Carlos Ruiz Cánovas [p], José Miguel Nieto [p], Nils Haneklaus [n,q,*]

[a] *École Nationale Supérieure des Mines de Saint Etienne, CNRS UMR, EVS, 5600, F42023 Saint Etienne, France*
[b] *OCP Group, Jorf Lasfar, El Jadida, Morocco*
[c] *Department INI, Geological Institute of Romania, Caransebeş Street, No. 1, Sect. 1, 012271 Bucharest, Romania*
[d] *Cepsa Exploracion Y Produccion Slu, Madrid, Spain*
[e] *Division Lafarge Plâtre, Avignon, France*
[f] *Institute of Geodynamics "Sabba S. Stefanescu" of Romanian Academy, 19-21 J.L. Calderon St., 020032, Bucharest, Romania*
[g] *Nuclear Centre of Energies, Sciences and Nuclear Techniques (CNESTEN), B.P. 1382, R.P. 10001, Rabat, Morocco*
[h] *Faculty of Sciences, Chouaib Doukkali University, El Jadida, Morocco*
[i] *College of Economics and Management, Yunnan Agricultural University, Kunming, China*
[j] *Department of Science and Technology – Philippine Nuclear Research Institute (DOST-PNRI), Commonwealth Ave, Diliman, Quezon City, 1101, Philippines*
[k] *Department of Ecology and Environmental Protection Technologies, Sumy State University, 40007 Sumy, Ukraine*
[l] *Department of Sustainable Technologies, Faculty of Tropical AgriSciences, Czech University of Life Sciences, Prague, 165 00, Prague, Czech Republic*
[m] *T. G. Masaryk Water Research Institute, 16000, Prague, Czech Republic*
[n] *Technische Universität Bergakademie Freiberg, Institute of Chemical Technology, Leipziger Straße 29, Freiberg, Germany*
[o] *High Throughput Multidisciplinary Research Laboratory (HTMR) and Institute of Science, Technology & Innovation (IST&I), Mohammed VI Polytechnic University (UM6P), Ben Guerir, 43150, Morocco*
[p] *University of Huelva, Department of Earth Sciences & Research Center on Natural Resources, Health & the Environment, 21071, Huelva, Spain*
[q] *Universität für Weiterbildung Krems, Td Lab Sustainable Mineral Resources, Dr.-Karl-Dorrek-Straße 30, 3500, Krems an der Donau, Austria*

ARTICLE INFO

Handling Editor: Cecilia Maria Villas Bôas de Almeida

Keywords:
Phosphogypsum
Circular economy
Radioactivity
Cleaner production

ABSTRACT

Nearly 300 million t of phosphogypsum (PG) are produced every year as a byproduct from phosphate fertilizer production worldwide. Approximately 58% of the PG are stacked, 28% are discharged in coastal waters and only 14% are further processed. This critical review provides an overview of the physical-chemical properties of PG produced from sedimentary and magmatic phosphate ore worldwide using various analytical tools. Results from more than 25 years of work on PG at École des Mines de Saint-Étienne are presented and critically discussed. In total PG samples from 67 industrial storage sites around the world and PG samples synthesized under different conditions in the laboratory have been considered. The low radioactivity present in PG (particularly PG produced from sedimentary phosphate rock) was identified as the main challenge to using PG as a raw material in construction. Water-soluble and volatile chemical compounds were identified as the main challenge to environmentally sound PG management. Although PG does (in most cases) not pose an immediate threat to the environment the authors recommend processing all PG instead of storing or disposing it, to eliminate potential long-term risks and utilize a relevant secondary resource.

* Corresponding author. Td-Lab Sustainable Mineral Resources, University for Continuing Education Krems (UWK), Dr.-Karl-Dorrek-Straße 30, 3500 Krems an der Donau, Austria.
E-mail address: nils.haneklaus@donau-uni.ac.at (N. Haneklaus).

https://doi.org/10.1016/j.jclepro.2023.137561
Received 24 February 2023; Received in revised form 16 April 2023; Accepted 22 May 2023
Available online 23 May 2023
0959-6526/© 2023 The Author(s). Published by Elsevier Ltd. This is an open access article under the CC BY license (http://creativecommons.org/licenses/by/4.0/).

1. Introduction

Circular economy considerations are gaining more and more momentum among practitioners and scholars (Corona et al., 2019; Kirchherr et al., 2017) putting pressure on the extractive industries to also move away from a linear economy model to a more circular one. The nature of mining obviously makes this challenging and circular economy considerations in mining usually focus on minimizing natural resource extraction and residual waste (Kinnunen and Kaksonen, 2019; Upadhyay et al., 2021) with a strong focus on waste, byproducts or mine tailings (Asr et al., 2019; Ojeda-Pereira and Campos-Medina, 2021).

Phosphogypsum (PG) is the primary byproduct generated during the production of phosphoric acid, an intermediate product in phosphate fertilizer production, from calcium phosphate (apatite) ore. PG also exists in very small amounts in nature where it is the result of natural guano processes as they took for instance place in the Cioclovina Cave located in the Şureanu Mountains in Romania (Onac et al., 2002). Nearly 300 million t PG are produced per year (Bouargane et al., 2023; Qin et al., 2023) of which 58% are dry- or wet stacked (Fuleihan, 2012), 28% are discharged into coastal waters, and only 14% are reused (Rutherford et al., 1994). It is also noteworthy that there are more than 3 billion t (estimates in the literature usually range from 3 to 8 billion t) additional PG stacks worldwide (Chernysh et al., 2021; Hermann et al., 2018; IAEA, 2013; Pliaka and Gaidajis, 2022; Tayibi et al., 2009).

Specifically, PG is generated at the stage of wet-phosphoric acid (WPA) manufacturing at which phosphate rock (pre-concentrated phosphate ore) is digested with sulfuric acid at approximately 80 °C as shown in Eq. (1) and schematically in Fig. 1.

$$\left[Ca_3(PO_4)_2\right]_3 CaF_2 + 10H_2SO_4 + 20H_2O = 6H_3PO_4 + 10(CaSO_4 2H_2O) + 2HF \quad (1)$$

The WPA process with sulfuric acid makes it possible to obtain PG in the form of a dihydrate ($CaSO_4{\cdot}2H_2O$) while other processes lead to the production of a hemi-hydrate ($CaSO_4{\cdot}0.5H_2O$) or an anhydrite ($CaSO_4$). The attack of one t phosphate rock is usually done with 0.6 t of concentrated sulfuric acid that generates approximately 0.4 t of phosphoric acid and 1.2 t of PG (Chang and Mantell, 1990; Hakim, 1997; van Selst et al., 1997).

The importance of calcium sulfate dihydrate ($CaSO_4{\cdot}2H_2O$) in industrial and agricultural fields as well as potential environmental risks associated with PG stacking (Tayibi et al., 2009) and PG disposal in coastal waters (Aoun et al., 2015; Belahbib et al., 2021; Ben Salem and Ayadi, 2017; Boudaya et al., 2019; El Zrelli et al., 2015; Jia et al., 2022) has increased interest in considering PG no longer a waste, but a byproduct of WPA production that could be utilized in construction to substitute natural gypsum (Aagli et al., 2005; Abu-Eishah et al., 2000; Burnett et al., 1996; Cárdenas-Escudero et al., 2011; Elkanzi and Chalabi, 1991; Haneklaus et al., 2022; Mulopo and Omoregbe, 2012).

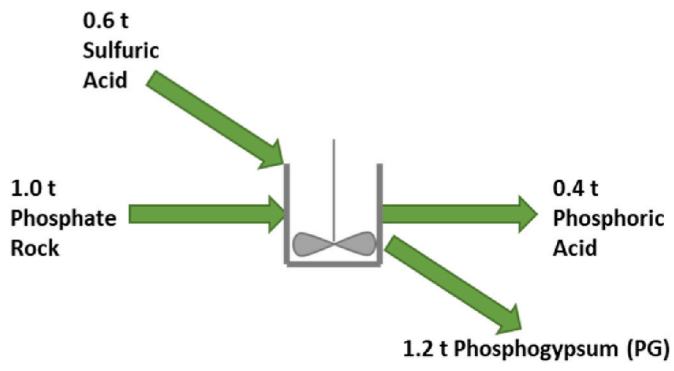

Fig. 1. Overview and mass balance of phosphoric acid and phosphogypsum production from phosphate rock with sulfuric acid.

In addition, phosphate ore can contain elevated concentrations of valuable trace elements in the form of rare earths (Akfas et al., 2023; Cánovas et al., 2016; Chen and Graedel, 2015; Emsbo et al., 2015; Ramirez et al., 2022) and uranium (Haneklaus, 2021). During WPA production with sulfuric acid uranium largely (>80%) transfers to the phosphoric acid product while the rare earths largely (>80%) transfer to the PG matrix (Rutherford et al., 1994). Circular economy considerations in phosphate rock processing (Scholz and Wellmer, 2018), increased demand for uranium (Gabriel et al., 2013; Mudd, 2014) and rare earths (Balaram, 2019; Liu and Chen, 2021), as well as geopolitical supply risks (Habib and Wenzel, 2014; Jyothi et al., 2020; Mancheri et al., 2019) have spurred research investigating potential rare earths recovery from PG (Cánovas et al., 2019; Kandil et al., 2010; Lütke et al., 2022; Rychkov et al., 2018; Walawalkar et al., 2016) and techno-economic feasibility of uranium recovery from WPA (Beltrami et al., 2014; López et al., 2019; Shang et al., 2021; Tulsidas et al., 2019; Ye et al., 2019). Industrial processes for uranium recovery from WPA are available and were used in the United States in the 1980s until decreasing uranium prices made the practice unprofitable in the 1990s (Haneklaus et al., 2017a, 2017b; Kim et al., 2016; Steiner et al., 2020). It is noteworthy that direct leaching approaches for rare earths and uranium recovery from phosphate ore are also under investigation (Al Khaledi et al., 2019; Banihashemi et al., 2021; Guzmán et al., 1995; Roshdy et al., 2023) and uranium concentrations in phosphate ore can reach concentrations exceeding those of commercial uranium mines (Mwalongo et al., 2022). If successful, direct leaching approaches could limit the radioactivity of PG considerably and thus make the material available as a secondary raw material in construction.

Despite the interest in rare earth element (REE) recovery, PG still largely (about 96 wt%) consists of gypsum. Depending on the type of the phosphate ore, traces of Cd, Zn, Pb, Hg, Zr, Cu, Ba, REEs, Y, Th, U and ^{226}Ra (which gives off ^{222}Ra) are the most common and relevant trace elements in PG. The radioactivity of the PG is usually 3–4 times higher than that of the phosphate ore (Arhouni et al., 2022; Diwa et al., 2021; El-Bahi et al., 2017; Hakkar et al., 2021; Qamouche et al., 2020). In Table 1 the radioactivity of PG is compared to concrete, ceramic bricks and natural gypsum. While the values for ^{4} K are smaller in the case of PG, the radioactivity for ^{266}Ra and ^{232}Th can be 10 to 100 times higher than those of the conventional building materials.

During WPA production, PG usually settles in a slurry and the resulting acidic process waters are recycled. The recycling of the process waters further concentrates the trace elements in the PG and the material is acidic because of the acids involved in the WPA production process. In addition, fluorine from the phosphate ore is also present.

During dry stacking of PG rainwater and remaining process waters can combine to form a hydraulic head that forces the infiltration of the acidic stack water into underlying aquifer systems or surrounding water bodies (Al-Hwaiti et al., 2010; Bituh et al., 2013; Borilo et al., 2012; El Zrelli et al., 2019; Lysandrou and Pashalidis, 2008; Pérez-lópez et al., 2016; Pérez-López et al., 2015; Zhou et al., 2023). Besides, fine dust from the powder-like PG stacks can be emitted causing respiratory problems (Adeoye et al., 2021; Lütke et al., 2020; Silva et al., 2022). As a result, these wastes may be harmful to the environment and, in the long term, induce health problems to local populations.

PG represents both an environmental problem and an opportunity

Table 1
Radioactivity of PG compared with the radioactivity of some building materials.

Products	^{266}Ra αBq/kg Radon gas	^{232}Th αBq/kg Thoron gas	^{4} K γBq/kg	Index I = Ra/300 + Th/200 + K/3000
Concrete	25–50	20–50	200–1000	<0,3
Bricks	50	15	600–1000	<0,3
Gypsum	10–20	2–20	10–80	<0,2
PG	100–2000	15–200	15–80	>1

for valuable secondary resource recovery. Within the context of present-day regulations and circular economy considerations, the only reasonable way to dealing with this material is the development of sustainable practices for complete (zero-waste) utilization of PG.

Given the large amounts of PG tailings produced annually it is not surprising that a number of researchers have already investigated and reviewed potential zero-waste strategies for PG utilization (Bouargane et al., 2023; Cánovas et al., 2018; Y. W. Cao et al., 2021; Chernysh et al., 2021; El-Didamony et al., 2013; Fornés et al., 2021; IFA, 2020; Kulczycka et al., 2016; Mohammed et al., 2018; Qin et al., 2023; Rashad, 2017; Rosales et al., 2020; Saadaoui et al., 2017).

Although present in relatively small quantities by weight and volume the trace-elements (particularly the radioactive ones) associated with PG are usually the limiting factor to zero-waste PG utilization. The quantities of these trace-elements in the PG depends largely on the phosphate ores processed and the chemical processes (usually it is the WPA process with sulfuric acid) used for phosphoric acid production (Macías et al., 2017; Rutherford et al., 1995). A detailed knowledge of the trace-elements present in different PG stacks is thus of profound interest when developing zero-waste PG utilization strategies that should be applicable to a wide range of locations worldwide.

This critical review provides an overview of the physical-chemical properties of PG produced from sedimentary and magmatic phosphate ore worldwide. Results from more than 25 years of work on PG at École des Mines de Saint-Étienne (EMSE) are for the first time presented together and critically discussed. In total PG samples from 67 industrial sites around the world and PG samples synthesized under different conditions in the laboratory have been considered. The large sample set allowed the authors to draw new conclusions with regards to PG texture and morphology (Chapter 3.1), PG chemistry (Chapter 3.2), PG dehydration (Chapter 3.3) and PG synthesis (Chapter 3.4) that led to an improved discussion on PG circular economy considerations (Chapter 4).

2. Materials and methods

PG samples (67 in total) and phosphate rock samples for production of PG in the laboratory were provided by different phosphoric acid and phosphate fertilizer producing companies from around the world who anonymity was promised in exchange for samples. The samples were usually dried at low temperature to reduce the humidity and then analysed shortly after they were received. For this review we largely relied on the historic data and only analysed samples again if we felt data was incomplete or inconclusive. When PG samples are stored the samples humidity content can change. The storage, even over longer periods of time, should not affect the concentration of major elements and minor trace elements. Gamma ray spectroscopy was used for radioactivity measurements and inductively coupled plasma mass spectrometry (ICP-MS) was used to determine the concentration of trace elements in the PG. In addition, PG samples were analysed using inductively coupled plasma optical emission spectroscopy (ICP-OES), infrared (IR) spectroscopy, scanning electron microscope (SEM), thermogravimetric analysis (TGA) and X-ray diffraction (XRD).

3. Results and discussion

3.1. PG texture and morphology

The texture of PG depends on the production process, the particle size distribution of the phosphate rock (relative speed of H^+, SO_4^{2-} and Ca^{2+} ionization), the concentration of the phosphoric acid in the reactor slurry (the higher reaction speed, the higher the ion mobility) and the solid/liquid ratio. Hemihydrate processes operate with 3–5% lower solids content if compared with dihydrate processes. According to (Bilal and Caspar, 2004) five morphological groups can be differentiated and examples of these different groups are provided in Fig. 2.

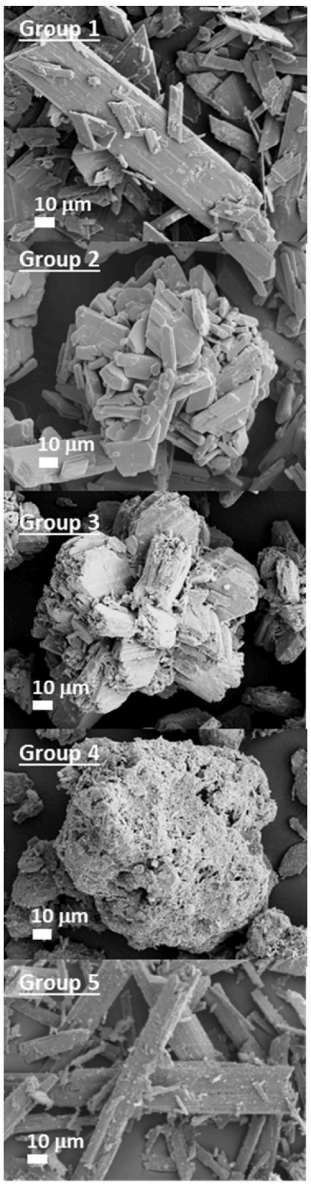

Fig. 2. PG types differentiated by their morphology and texture as rhombic type (Group 1), aggregate small rhombic type (Group 2), cluster type (Group 3), aggregate short needle type (Group 4) and needle type (Group 5).

Group 1 is characterized by needle-shaped crystals with a uniform distribution of fine needles and elongated platelets with sizes varying from 10 to 120 µm and crystallites typically ranging from 400 to 550 nm. The predominant phases in this group are gypsum, bassanite and traces of anhydrite. The needles tend to form monoclinic gypsum crystals. The particle size distribution of the phosphate rock feed in this group is usually as following: 160 µm (20–30%), 125 µm (30–40%), 80 µm (40–60%).

Group 2 is characterized by a texture of fine agglomerated needles that are 5–30 µm in size and crystallites ranging from 70 to 300 nm. Group 2 shows some of the characteristics of natural gypsum but the material is only agglomerated so that the cohesive forces, bonding the grains together is weaker. The concentration of the phosphoric acid in the reactor slurry in this group is usually as following: 30% P_2O_5 in phosphoric acid with 58.6% water. Further increasing the P_2O_5 content to 40% P_2O_5 and 44.7% water or even 52% P_2O_5 and 28.2% water will lead to smaller and more irregular crystallization of the PG.

PG of group 3 can be described as polycrystalline aggregates that are

in a disorderly manner. The crystals tend to form bunches that are sometimes referred to as "pink sand". The solid content in the slurry (solid/liquid ratio) is usually 30 vol%, if thick rhombic crystals are present or 22 vol% if needle type crystallization is given. The rhombic crystals are preferred for better filtration. In this context it is noteworthy that hemihydrate systems typically operate with 3–5% lower solids content than dihydrate systems.

The PG of group 4 differs significantly from the other groups. Here small grains are found that typically have a roundish, pebble like shape. In direct contrast, the PG of group 5 consists of very thin needle like crystals.

The texture of the PG is particularly important for its potential use as a building material. For example, in the plaster industry only certain gypsum crystal sizes are acceptable to produce plasterboards. Group 1, 2 and 5 are acceptable. On the other hand, group 3 and 4 cannot be used for plasterboard production but could be utilized in the cement industry or in agriculture. The texture and morphology also influence further processing of the PG in processes such as calcination.

3.2. PG chemistry

Phosphate rock is a mineral resource that contains phosphorus and is used as the raw material for the production of phosphoric acid, which is a key ingredient in fertilizer. It is mainly found in marine sedimentary deposits, igneous rocks, and guano. Approximately 75% of the global phosphate resources come from sedimentary phosphate rocks, while 20–25% are obtained from igneous deposits (Manning, 2008; Ptáček, 2016; Pufahl and Groat, 2017). Guano, despite its high phosphate content, cannot be used on a global scale as it is not available in enough quantities (Pufahl and Groat, 2017).

Practically, phosphoric acid can be produced from phosphate ore through two main routes: the wet process, which involves the use of strong mineral acids for decomposing of the phosphate, and the dry process, where the ore is heated in an electric furnace to produce elemental phosphorus as an intermediary (Abouzeid, 2008; Da Silva and Kulay, 2005). The wet process, in which phosphate rock is usually treated with sulfuric acid, is the prevalent way of manufacturing phosphoric acid today (Becker and others, 1989). This procedure leads to the production of considerable amounts of hydrated calcium sulfate, commonly referred to as PG (see simplified mass balance in Fig. 1). In accordance with the temperature as well as the phosphate and sulfate content of the solution, either calcium sulfate dihydrate (DH), hemihydrate (HH) or anhydrite (AH) is formed.

There are in fact two main wet processes that can be differentiated: single-stage processes and recrystallization processes. Single-stage processes consist of only one reaction-recrystallization step, regardless of the form of the obtained gypsum. The dihydrate (DH) and hemihydrate (HH) processes are the two most prevalent methods in single-stage procedures. The dihydrate (DH) process is widely used due to its simplicity and flexibility in the treatment of different types of phosphate rock and is therefore considered a reliable technique for phosphoric acid production on industrial scale (Abdelouahhab et al., 2022; Abu-Eishah and Abu-Jabal, 2001; Houghtaling, 1973). In this process, calcium sulfate in the form of gypsum (dihydrate: $CaSO_4$-$2H_2O$) is obtained at a temperature between 70 and 80 °C and moderate acid concentration. The energy efficiency of the DH process is lower due to the requirement to finely ground feed rock and the resulting dilute phosphoric acid, which requires additional energy for a subsequent concentration step. Phosphoric acid generated through the dihydrate process is generally denoted as wet phosphoric acid (WPA). The Hemihydrate process (HH) involves treating phosphate rocks at slightly higher temperatures (90–110 °C) (De Vreugd et al., 1994; Gioia et al., 1977; Jansen et al., 1984). The PG obtained by this method is contaminated with heavy metals and radioactive elements. The HH technique has the advantage of requiring less grinding, but, the recovery rate of P_2O_5 is slightly lower (Abu-Eishah and Abu-Jabal, 2001).

Recrystallization processes are intended to enhance the efficiency of recovering P_2O_5, including the production of a purer final filter cake and, in some cases, generating a higher-strength acid directly. These processes include hemihydrate-dihydrate (HDH), hemihydrate dihydrate recrystallization (HRC), and dihemihydrate (DH/HH) routes (Gobbitt, 2012; Koopman and Witkamp, 2000; Wang et al., 2021a, 2021b). In the HDH process, hemihydrate (HH) is produced first and then filtered from the strong pure phosphoric acid product. Subsequently, the HH is transformed into dihydrate (DH) through recrystallization, leading to higher process efficiencies. The primary disadvantages of the HDH technique are the corrosion caused by the higher temperatures in the reactors and the intricate nature of the process, that places a strain on the operating staff. The HRC starts with the decomposition of the phosphate rock under the same conditions as the hemihydrate process, but without filtration. Then, the product undergoes recrystallization to form dihydrate and is finally filtered to obtain the final product. This results in an acid with a slightly higher strength compared to that produced by the dihydrate processes. Furthermore, this technique leads to the formation of a pure dihydrate byproduct. The DH/HH process forms dihydrate (DH), which is filtered from phosphoric acid and then recrystallized to produce a pure hemihydrate (HH) product. The HH product can be used directly in the production of plasterboards. Over the last 20 years, the primary focus in WPA production has been the reduction of the energy costs. Despite low energy consumption per kilogram of P_2O_5 produced, the total cost is substantial due to the high overall production rates. The most energy-intensive step in the production of phosphoric acid, if the chemical and not the thermal route is chosen, is associated with the grinding of the phosphate rock. In fact, the processes that can handle coarser rock feeds (e.g., HH and HDH) have become more significant due to their overall lower energy consumption. Table 2 shows the average composition of PG from different industrial production processes. It is noteworthy that the individual production process influences the PG texture and morphology that was discussed in the previous chapter. It is, however, not possible to link the specific texture and morphology groups that were defined earlier (Group 1–5) directly to the specific WPA processes listed in Table 2.

Generally, the PG samples produced from sedimentary phosphate rock (s-PG) have higher SiO_2 contents than the PG samples produced from magmatic phosphate rock (m-PG) with the exception of Kola Peninsula PG samples that also have a high concentration of Na_2O (rock phosphate initials formed nepheline ($Na_3KAl_4Si_4O_{16}$)). The Y, Zr, Cu and Ba contents are much higher in m-PG resulting from treatment of igneous apatite than in those from the sulfuric treatment of sedimentary ores. Tunisian PG (an s-PG), for example, has relatively high levels of Cd, Hg and Zn (Abbes et al., 2020; Choura, 2007; El Zrelli et al., 2015; Rutherford et al., 1994). Approximately 80% of the Cd content passes preferably to the phosphoric acid (Rutherford et al., 1994). If clean sulfuric acid is used, the major components of the PG composition varies with the treatment of the phosphate rock while the trace elements mainly depend on the origin of the ore. Macías et al. (2017) describe well how sulfuric acid from pyrite roasting was used in the production of Huelva PG. This sulfuric acid actually added a number of trace elements to the PG that did not result from the phosphate rock itself showing that the acid used for the digestion can also be an additional source of impurities. Radioactive elements, most notably ^{226}Ra, ^{232}Th, ^{40}K result in the typical radioactivity indexes ($I = (Ra/300) + (Th/200) + (K/3000)$) of 1.33–2.59 for s-PG and the mixed PG (m-PG and s-PG). m-PG (particularly m-PG from Russia and some PG from China) typically shows relatively low radioactivity indexes of 0.24–0.45. m-PG and also mixed PG thus tend to show radioactivity indexes ($I < 1$) that theoretically allow for the use of the material in construction as established by the International Commission on Radiological Protection (ICRP) (Calderón-Morales et al., 2021; Campos et al., 2017; Kuzmanović et al., 2021). In practice however, the material is often not used since it is harder to sell than a natural raw material that might show lower

Table 2
Average PG composition from industrial production.

Phosphate Rock	Sedimentary				Magmatic	Mixed
Process	HDH Hitashi	HDH Hydro Agry	DH Jacob	DH Prayon (S)	DH Prayon (M)	HRC Kemira
Loss of ignition (1000 °C)	17.78%	20.65%	20.68%	21.10%	19.71%	20.72%
Combined moisture	12.74%	22.91%	16.31%	NR	NR	NR
Purity (sample dried at 250 °C)	93.27%	94.87%	91.83%	NR	95.56%	NR
pH (5% solution in distilled water)	3.9	4.4	3.3	NR	NR	NR
Major elements						
CaO%	30.53%	33.65%	33.73%	35.20%	35.85%	36.42%
SO_3%	44.83%	45.82%	42.50%	44.47%	43.49%	NR
SiO_2%	4.70%	6.82%	4.38%	5.13%	2.39%	3.25%
Al_2O_3%	0.08%	0.14%	0.36%	0.19%	0.36%	ND
Fe_2O_3%	0.18%	0.06%	0.12%	0.18%	0.25%	0.03%
P_2O_5%	1.31%	0.28%	0.78%	0.52%	0.70%	0.38%
Soluble P_2O_5	0.23%	NR	NR	0.37%	0.08%	0.02%
Na_2O%	0.06%	0.06%	0.08%	0.04%	0.07%	0.02%
K_2O%	0.03%	0.02%	0.10%	0.01%	0.05%	0.02%
TiO_2%	0.03%	0.02%	0.03%	0.03%	0.29%	ND
MgO%	0.04%	0.07%	0.02%	<0.01%	0.04%	ND
MnO%	0.01%	0.01%	NR	<0.01%	0.01%	ND
F%	0.55%	0.61%	0.64%	0.45%	0.55%	0.05%
Soluble F	0.21%	0.35%	0.11%	0.31%	0.24%	0.11%
CO_2%	0.21%	0.56%	0.39%	0.35%	0.28%	0.12%
Organic C	0.01%	0.11%	0.05%	0.04%	0.02%	0.01%
Chloride as Cl	1.78 mg/L	1.86 mg/L	0.88 mg/L	2.4 mg/L	NR	NR
Nitrate	8.70 mg/L	6.83 mg/L	6.86 mg/L	10.02 mg/L	NR	NR
Trace elements						
As	NR	NR	NR	2 ppm	NR	NR
Co	1 ppm	1 ppm	1 ppm	<1 ppm	5 ppm	1 ppm
Zn	49 ppm	48 ppm	34 ppm	44 ppm	14 ppm	8 ppm
Pb	6 ppm	2 ppm	2 ppm	4 ppm	<1 ppm	ND
Cd	1 ppm	2 ppm	2 ppm	3 ppm	<1 ppm	ND
Ni	3 ppm	2 ppm	1 ppm	4 ppm	1 ppm	ND
V	4 ppm	2 ppm	4 ppm	2 ppm	7 ppm	1 ppm
Cr	4 ppm	5 ppm	7 ppm	14 ppm	4 ppm	3 ppm
Cu	9 ppm	60 ppm	1 ppm	33 ppm	5 ppm	10 ppm
Ba	76 ppm	109 ppm	150 ppm	53 ppm	207 ppm	39 ppm
Sr	569 ppm	801 ppm	402 ppm	NR	7692 ppm	2099 ppm
Th	1 ppm	1 ppm	1 ppm	3 ppm	42 ppm	4 ppm
U	2 ppm	5 ppm	3 ppm	<1 ppm	52 ppm	8 ppm
Rare earths (including Y)						
Y	18 ppm	27 ppm	72 ppm	140 ppm	133 ppm	27 ppm
La	9 ppm	14 ppm	39 ppm	49 ppm	1215 ppm	165 ppm
Ce	10 ppm	15 ppm	20 ppm	31 ppm	1998 ppm	246 ppm
Nd	7 ppm	11 ppm	25 ppm	37 ppm	921 ppm	NR
Sm	1 ppm	2 ppm	6 ppm	NR	NR	NR
Eu	<1 ppm	1 ppm	1 ppm	2 ppm	NR	NR
Gd	1 ppm	2 ppm	7 ppm	10 ppm	NR	NR
Tb	<1 ppm	<1 ppm	1 ppm	3 ppm	NR	NR
Dy	1 ppm	2 ppm	7 ppm	NR	NR	NR
Ho	<1 ppm	<1 ppm	2 ppm	2 ppm	NR	NR
Er	1 ppm	1 ppm	5 ppm	6 ppm	NR	NR
Tm	<1 ppm	<1 ppm	1 ppm	NR	NR	NR
Yb	1 ppm	1 ppm	4 ppm	8 ppm	NR	NR
Lu	<1 ppm	<1 ppm	1 ppm	1 ppm	NR	NR
$\sum$ REEs + Y	49 ppm	78 ppm	180 ppm	289 ppm	3960 ppm	438 ppm
Radioactivity						
^{226}Ra	211 Bq/kg	596 Bq/kg	414 Bq/kg	562 Bq/kg	267 Bq/kg	NR
^{232}Th	5 Bq/kg	<7 Bq/kg	5 Bq/kg	32 Bq/kg	185 Bq/kg	NR
^{235}U	<7 Bq/kg	<16 Bq/kg	73 Bq/kg	<9 Bq/kg	261 Bq/kg	NR
^{40}K	<10 Bq/kg	<26 Bq/kg	60 Bq/kg	<12 Bq/kg	NR	NR
Radioacativity Index I	0.73	1.99	1.71	2.03	NR	NR

NR: Not reported; ND = not detected.

radioactivity, better strengths when processed and pose much lower legal risks to producing companies that might have to adjust to changing national regulations. Nevertheless, developments in PG treatment have been made to further decrease the levels of radioactivity and impurities. The treatment methods vary and may include washing, filtration, calcination, neutralization, leaching, and purification, among others, to remove impurities and further reduce the radioactivity levels. The specific process used depends on the composition of the PG and the required end use. The challenge of resolving the crystallization of thorium nesosilicate ($ThSiO_4$), which is a highly radioactive substance, in m-PG remains unresolved though. The radioactivity measurements on different sites have shown that fine particles are richer in radon than fractions above 30 μm. Some PGs that were previously washed, showed a decrease in levels of heavy metals, Th, REEs, P_2O_5, Na_2O and K_2O.

The contents of major impurities in PG vary according to the process type used, while the trace concentrations would depend directly on the nature of the initial phosphate rock (Rutherford et al., 1994). Only As, Ba, Cd, Cr, Pb, Hg, Se and Ag are classified as toxic elements by the United States EPA (Environmental Protection Agency). Their content in PG is usually less than the tolerated limit though. The fate of major and

trace elements in gypsum can be attributed to many processes such as precipitation in a fairly pure mineral phase, inclusions of liquids, co-precipitation, formation of solid solutions and surface adsorption of organic compounds or minerals. Free phosphoric acid, unreacted phosphates, sodium hexafluorosilicate, sodium sulfate, fluorosilicic acid H_2SiF_6 and organic compounds adhere to the surface of the gypsum crystals.

PG may contain heavy metals (Burnett et al., 1996; Hamdona et al., 1993) such as Pb, Cd, Hg, Zn and Cu (Al-Masri et al., 2004; Cossa et al., 2001; Garrido et al., 2005; Van Der Sluis et al., 1986) with Cu usually being the most abundant one (117 ppm). The Cd (usually 1 ppm) of the Syrian PG is in 45–58 μm fine fractions while most heavy metals (Cr, Co, Zr, Cu, Pb, Z n, Ag, Ni, Cd and V) are found in the particle size fraction less than 20 μm (Rutherford et al., 1996; Fávaro, 2005).

REEs (except Ce), Th and Ba are essentially in a residual phase which corresponds to a small fraction of rock phosphate or monazite: (Ce, La, Nd, Th)PO_4 and has insoluble compounds such as phosphates and silicates (Santos et al., 2006). 60–80% of the REEs (especially the light ones: La to Sm) present in the phosphate rock are found in the PG. In both the dihydrate or hemihydrate process the heavy REEs (Gd and Lu) migrate into the phosphoric acid. REEs, Y, Ba and Sr are typically found in the fine fraction (<20 μm) (Fávaro, 2005).

The m-PGs have higher strontium and rare earths contents (La and Ce mainly but also Pr, Eu, Dy, Er and Lu) than s-PGs. In this work it was possible to draw a border zone, where the Sr/Ca ratio is approximately 0.0057 (Sr/Ca <0.0057 = s-PG and Sr/Ca> 0.0057 = m-PG) (Bilal et al., 2010) (see Fig. 3, Fig. 4 and Fig. 5).

Lanthanides retard the growth rate of gypsum crystals on all sides (preferably that with miller indices (011) of needles for cerium) except for (−111) (Ce^{3+}> La^{3+}> Eu^{3+}> Er^{3+}) because the ionic radius of lanthanides such as cerium (128pm) is closer to that of calcium (126pm) than lanthanides such as erbium (114pm)) (Koopman and Witkamp, 2002). In addition, Ce^{3+} and Na^+ form a solid solution with the hemihydrate during crystallization [$(Na,Ce)(SO_4)_2.H_2O$ + $CePO_4.0.5H_2O$] – $CaSO_4.0.5H_2O$. This stabilizes the structure of the hemihydrate and slows down the recrystallization of the dihydrate (Rutherford et al., 1994).

The other elements which can be substituted in the structure of the gypsum are Cd, Sr, Mg, Na, K, Cl and Se. Cd^{2+} ions can replace Ca^{2+} ions because they have the same charge and very similar ionic radii (1.12A and 1.07A respectively). The incorporation of Cd^{2+} increases with increasing H_2SO_4 (Rutherford et al., 1994).

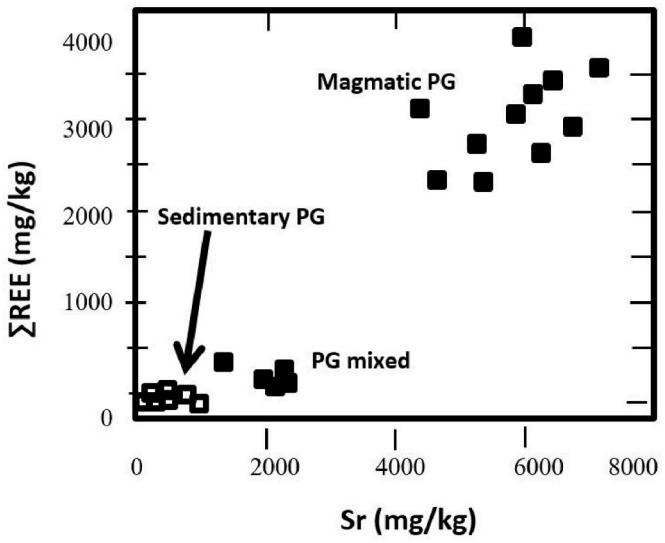

Fig. 3. Distribution of PG (Magmatic PG and Sedimentary PG) in sum of REE versus Sr diagram.

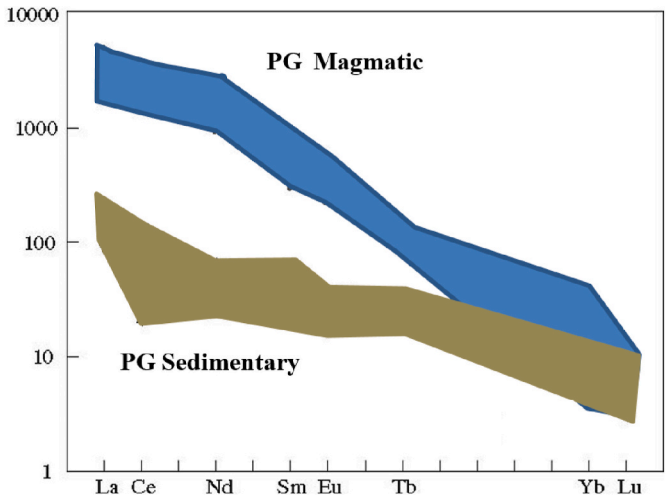

Fig. 4. Distribution of PG (s-PG and m-PG) in Chondrite normalized diagram.

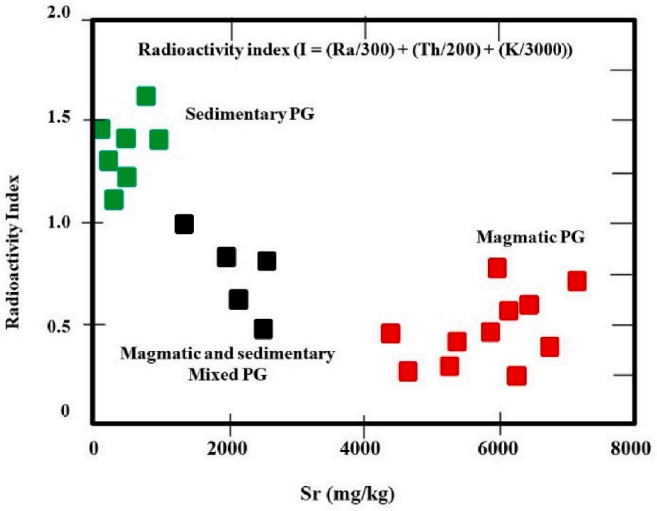

Fig. 5. Radioactivity index of PG (s-PG, m-PG and mixed phosphate PG) versus Sr diagram.

The s-PGs usually have higher SiO_2 contents than the m-PGs with the exception of the PG produced from phosphate rock from the Kola Peninsula (Russia) (a m-PG that also has high Na_2O contents because they are made up of nepheline ($Na_3KAl_4Si_4O_{16}$)). Silica exists as amorphous SiO_2, quartz or SiO_2-containing minerals (Elkanzi and Chalabi, 1991; Rutherford et al., 1994). The selenium may be found in the form of $CaSeO_4.2H_2O$ in the PG (Kruger and Abriel, 1991). Fluorides precipitate in the form of complex crystalline salts, depending on the concentrations of Al, Si, Mg, Na, Ca and sulphates dissolved in the acid. The most common are calcium fluorosilicate and calcium fluoride. During the process of manufacturing phosphoric acid, silicon increases the growth of the gypsum crystals along the c-axis and prevent the formation of aggregates because it tends to dissolve fluorine, which does not syncrystallize in the PG. This therefore shows normal acicular growth.

Aluminum and silica tend to form complexes with fluorides and therefore modify the distribution of ionic species ($6F^- = SiF_6^{2-}$ or AlF_6^{3-}). When the alkali concentration is low, then chukhrovite: $Ca_4(SO_4)(AlF_6)SiF_6).12H_2O$ (whose structure has been described by (Mathew et al., 1981)) can precipitate. For high dissolved aluminum concentrations, fluorine precipitates in the form of cryolite: $(Na, K)_3AlF_6$. The presence of magnesium changes the fluorine precipitation mechanism. Specifically, the $MgSiF_6.6H_2O$ phase appears. This group of fluorosilicates

crystallize in acicular form, which helps to improve the filterability of calcium sulfate. When F, Mg, Na and Al are present, ralstonite: $Na_xMg_xAl_{2-x}$ (F, OH)$_6H_2O$ (x between 0.2 and 1.0 and the F/OH molar ratio between 3 and 1) is frequently formed (Lehr et al., 1966). Fluorite and fluorapatite may be the solids controlling the solubility potentials of fluorine in PG. The study of the PO_4-SiO_2-F system has shown an interdependence between PO_4^{3-} and F^- because they are surely associated with the same phase, apatite ($Ca_5(PO_4, CO_3)_3(F, OH)_2$) which reprecipitates between F^- and SiO_2 because they would form an alkaline hexa-Fluorosilicate ($(Na, K)_2SiF_6$) (Burnett and Elzerman, 2001). The length/width ratio (L/l) varies depending on the impurity present in the PG. Indeed, the presence of fluorides (up to 2.09–2.80% in F^-) or SiO_2 (0.9–3.0%) leads to an increase of L/l while this ratio remains unchanged with impurities such as CO_2 (1.5–4.6%) and Fe_2O_3 (0.17–0.48%) or decreases slightly with Al_2O_3 (0.15–0.40%).

Dicalcium phosphate, monosodium sulfate and fluorophosphate can also enter the structure of gypsum. A solid solution exists between the dicalcium phosphates because the HPO_4^{2-} ions replace the SO_4^{2-} ions in the gypsum structure because these 2 ions have the same size, molar mass and charge (Van Der Sluis et al., 1986). This substitution of phosphates in the gypsum network during acidification is reduced with a high concentration of sulphates, longer attack times of the phosphate rock, higher reaction temperatures and a large percentage of solids. The incorporation of HPO_4^{2-} decreases when H_2SO_4 increases. HPO_4^{2-} ions can be incorporated into the gypsum structure thus forming ardealite ($Ca(SO_4)_{1-x}(HPO_4)_x.2H_2O$) where x = 0.5 (Freyer and Voigt, 2003). One method to differentiate PG from synthetic gypsum is for instance the analysis by IR spectroscopy. PG as an additional band at 840 cm^{-1} relating to the absorption of the H_2PO_4 group (Hanna et al., 2009) that cannot be observed in case of synthetic gypsum (Sebbahi et al., 1997).

El Moussaouiti et al. (1996) observed the appearance of a band at 836 cm^{-1} generated by phosphate ions and the increase in intensity of that at 1094 cm^{-1} corresponds to the superposition of the vibrations of SO_4^{2-} and HPO_4^{2-}. It was then proven (Guilhot et al., 1974) that by IR spectroscopy, it is possible to highlight the syncrystallized HPO_4^{2-} ions (836 and 1015 cm^{-1}), HPO_4^{2-} from the brushite phase (872 cm^{-1}) and syncrystallized FPO_3^{2-} (766 and 1025 cm^{-1}). They can be measured (the heights of these bands depend on the content of syncrystallized ions) (Guilhot et al., 1974). Gypsum crystals were observed to be needle-like as long as the molar fraction of syncrystallized HPO_4^{2-} ions does not exceed 0.07 to 0.085. Beyond this value, the products appear in the form of lamellae groups in flower-like forms (Guilhot et al., 1974). EDS analyzes (energy dispersive spectroscopy) do not show the presence of phosphorus in PG (El Moussaouiti et al., 1996).

The complexes containing the AlF_5^{2-} ions retard the growth of gypsum crystals because they replace the SO_4^{2-} ions and are mainly adsorbed on the faces (011) and (−111) hence a decrease in the L/l ratio of the crystals can be observed. The presence of aluminum fluorides causes also the formation of small agglomerated crystals, having a hexagonal structure (Koopman and Witkamp, 2002; Martynowicz, 1994; Martynowicz et al., 1996a, 1996b). From the Al content of the phosphate rock and the values of the aluminum distribution coefficients, it is possible to know the aluminum concentration during the hemihydrate process and the probability that difficult to filter dihydrate crystals are formed. The applicability of different phosphate rocks, in terms of their Al content, can be determined (Martynowicz et al., 1996b). The hemihydrate obtained by calcining gypsum containing this co-crystallized species has a setting-time which is less easy to control by adding a setting retarder than the pure hemihydrate (Kitchen, 2007). During the phosphoric acid manufacturing process, the presence of aluminum limits the growth of gypsum along the c-axis and promotes the formation of aggregates. The presence of carbonates can lead to the formation of rapidcreekite ($Ca_2(SO_4)(CO_3)_4H_2O$) (Dydo et al., 2003).

3.3. PG dehydration

Efforts should focus on impurities, which play an important role in the hydration of PG to use as substitutes for natural gypsum. Indeed, the s-PG shows conductometric curves highly variable and late stabilization of conductivity (2.9 mS/cm) after 16 min and up to 32 min. Some of the s-PGs are characterized by a late conductivity stabilization, greater than 40 min and the conductivity at a high value of 4.1 mS/cm. Some of S-PGs can further be characterized by a late conductivity stabilization, greater than 40 min and the conductivity at a high value of 4.1 mS/cm (see Fig. 5).

The S-PG has impurities that slowly release and can result in an increase of the setting time (Fig. 6). The conductivity stabilization time (setting time) reduced after many washings of s-PG prior to dehydration. Experimental work in the EMSE laboratory (Bard and Bilal, 2011; Bilal et al., 2014; Bourgier, 2007; Laborde, 2002) showed that the hydration depends mainly on the presence of P_2O_5 in the PG, which was also confirmed more recently by others (see for instance (Jia et al., 2021; Liu et al., 2020)). This effect disappeared when heating the PG at 160 °C during which a reversal of the conductometric curves could be observed with significant reduction of the setting time (Fig. 6). Excellent work on this was also carried out by (Geraldo et al., 2020) for PG from Brazil as well as (Cao et al., 2022; W. Y. Cao et al., 2021) and (Li and Zhang, 2021) for PG from China. The relatively low required temperatures led to first experiments to consider waste heat (Mittal and Rakshit, 2020) or solar power (Palla et al., 2022) for treatment of PG. Experimental laboratory studies have also shown that a treatment consisting of washing with dilute citric acid solutions (Singh, 2002), oxalic acid solutions (Cai et al., 2021) or sulfuric acid solutions (Bilal et al., 2010, 2014) helped reducing soluble P_2O_5 in the PG considerably.

3.4. PG synthesis

To better understand the morphology, texture, and presence of impurities in PG various syntheses of PG and gypsum were carried out. The first lesson learnt is that the composition and morphology depend on the starting composition of the phosphate ore and the concentrations of the sulfuric acid during the acid attack and the washing that follows. During the acid attack little mobile elements are found in or with the PG such as P_2O_5 and F in solid or dissolved form as: $Ca(H_2PO_4).2H_2O$, Ca_3PO_4, CaF_2, $CaHPO_4.2H_2O$ (brushite), $CaFPO_3.2H_2O$; and HPO_4^{2-}, FPO_3^{2-} ions and AlF_5^{2-} (Kitchen, 2007; Martynowicz et al., 1996a) co-crystallized in PG. During washing, several salts and acids are not completely eliminated ($H_2PO_4^-$, SiF^{6-} or F^-, Na^+ and K^+).

The excess of sulfuric acid and temperature in the acid attack plays an important role on the texture and morphology of the PG that has already been discussed in Chapter 3.1 and is further illustrated in Fig. 7. The excess sulfuric acid in the reactor slurry is the most effective factor governing the quality of the crystallization. With very low sulfuric acid content, only small diamond-like crystals are produced (Bard and Bilal, 2011). As the sulfate levels increase, the crystal size increases and the shape of the crystals stretches out most of the time, eventually becoming needle-like. The level of sulfuric acid is also responsible for the syn- or co-crystallization of the P_2O_5.

The crystal structure of brushite is similar to that of gypsum despite not being isostructural. Both minerals belong to the monoclinic system, but they have different space groups (Cole and Lancucki, 1974; Curry and Jones, 1971). This similarity makes the investigation of the brushite-gypsum system by XRD challenging. In fact, the intense peaks that correspond to the reflexion 020 ($2\theta = 11.7°$) of brushite and gypsum are indistinguishable (Roode-Gutzmer and Strydom, 1999). However, to differentiate these two phases the peaks at $2\theta = 20.7°$ for gypsum and $2\theta = 21.0°$ for brushite should be considered. The two peaks are only discernible for brushite contents greater than 1% in the gypsum and brushite mixture.

On the other hand, XRD analysis can reveal the presence of a new

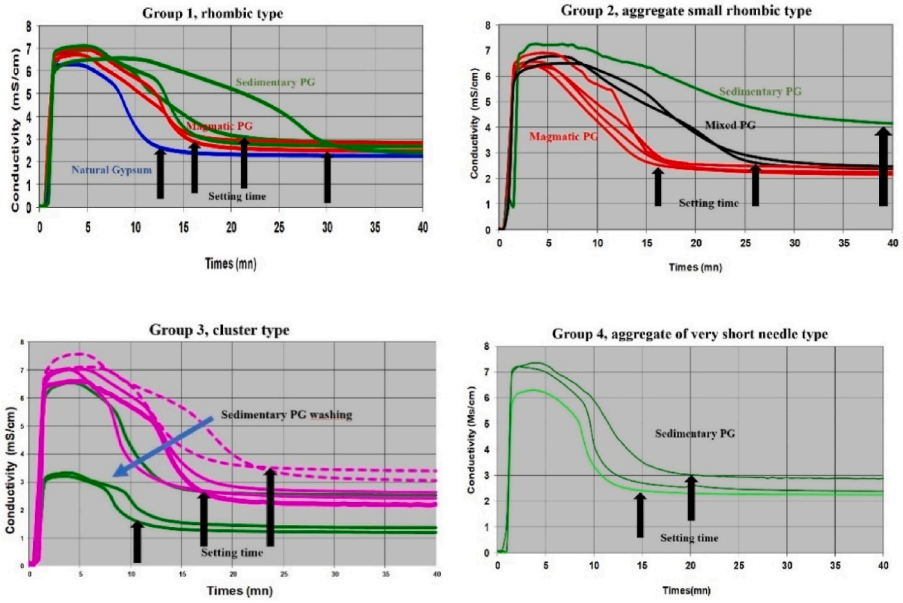

Fig. 6. Conductometric curves of different PGs and stabilization time of conductivity (setting time).

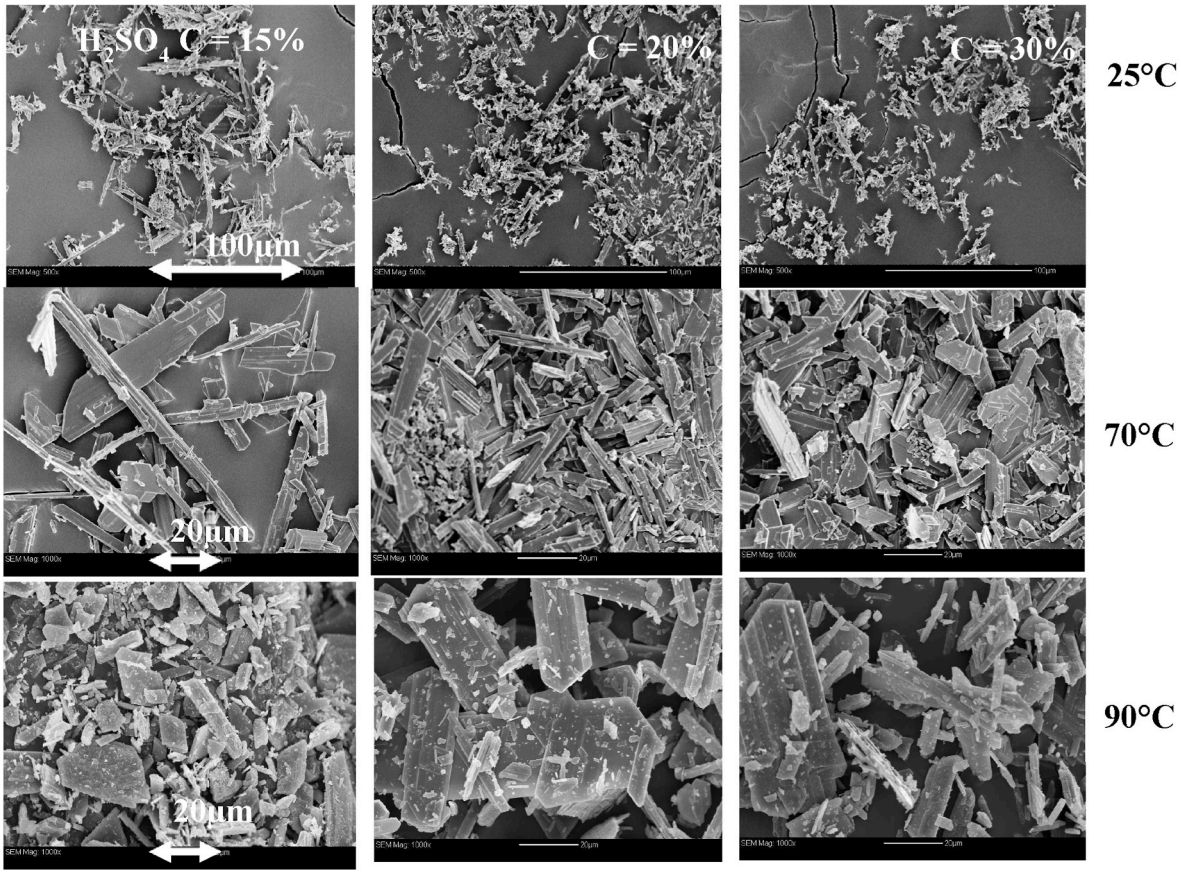

Fig. 7. Variation of the texture of the gypsum according to the content of H_2SO_4 and the temperature.

phase, ardealite ($Ca_2(SO_4)(HPO_4).4H_2O$), if the phosphate ion content is above 7% (Fig. 8). For HPO_4^{2-} contents between 40% and 55%, the gypsum disappears and only the ardealite ($Ca_2(SO_4)(HPO_4).4H_2O$) phase remains. For HPO_4^{2-} contents between 55% and 95%, ardealite coexists with brushite but beyond that only brushite is present. Rinaudo et al. (1994) obtained the same order of appearance of the phases according to the variation of the contents of HPO_4^{2-} but they did not see the demixing of ardealite into ardealite and brushite after 55% of the ion HPO_4^{2-}.

In fact, the dehydration of brushite is less known than that of gypsum. Fig. 9 highlights the behaviour of brushite when it has been calcined at different temperatures. For temperatures between 25 and

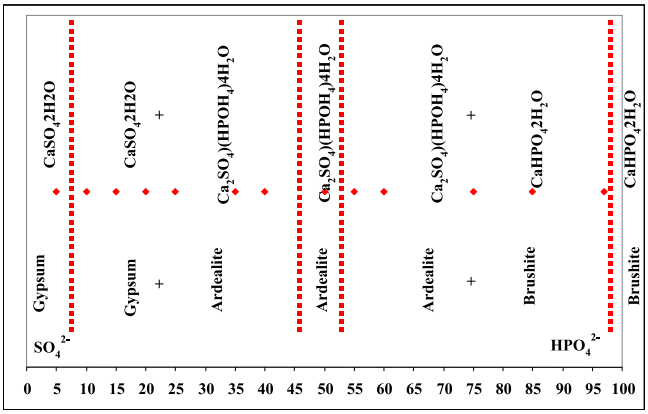

Fig. 8. Order of appearance of the phases (XRD analyzes) as a function of the variation in the HPO_4^{2-} contents.

250 °C, only the brushite $CaHPO_4.2H_2O$ and monetite $CaHPO_4$ phases were observed. At 250 °C, the initial brushite transformed into monetite after losing its structural water. The $Ca_3(PO_4)_2$ and $Ca(H_2PO_4).H_2O$ phases were not detected by XRD. According to Lang Dupont (1985), it is impossible to obtain pure anhydrous calcium phosphate since before total dehydration, calcium pyrophosphate ($Ca_2P_2O_7$) begins to form. There is always a superposition of the two reactions. During the dehydration of the gypsum-brushite mixtures, the transformation of anhydrite III into anhydrite II occurs at higher temperatures than for pure gypsum. The brushite present in the mixture is transformed at 150 °C into two phases (Fig. 10): 24% brushite and 76% monetite (semi--hydrated phase). This brushite differs from the first by its physico-chemical characteristics.

In situ XRD analysis revealed that ardealite ($Ca(HPO_4)(SO_4).4H_2O$) was decomposed during heat treatment into brushite ($CaHPO_4.2H_2O$), monetite ($CaHPO_4$) and bassanite ($CaSO_4.0{,}5H_2O$) (see Fig. 11). At a temperature above 150 °C, the bassanite was transformed into anhydrite III, while at 250 °C, brushite was entirely replaced by monetite. Subsequently, between 250 °C and 350 °C, the appearance of stable anhydrite II ($CaSO_4$) and amorphous calcium pyrophosphate ($Ca_2P_2O_7$) was observed. This explanation of the dehydration of ardealite is consistent with that of Balenzano et al. (1984) and Secco et al. (2015).

The infrared absorption spectra of the gypsum-brushite mixtures are shown in Fig. 12 and the characters and intensities of the absorption bands obtained on the different gypsum and brushite mixtures are given in Table 3. The band assignments are in agreement with the work of Dumitras et al. (2004) which was based on previous work (Berry and Baddiel, 1967; Murat, 1982; Petrov et al., 1967; Tortet et al., 1996; Trpkovska et al., 1999). Infrared absorption spectra of the mixture containing 50% gypsum and 50% brushite ($CaHPO_4.2H_2O$) show the characteristic bands of gypsum and brushite. They are very different from those of ardealite ($Ca_2(SO_4)(HPO_4).4H_2O$). IR can thus be used as a relatively simple method to distinguish the mechanical mixtures of gypsum-brushite of a phase of the ardealite type containing in equal proportions HPO_4^{2-} and SO_4^{2-}.

Brushite in a gypsum-brushite mixture, is detectable in the infrared spectrum by the absorption band 872 cm^{-1} (see Fig. 12) corresponding to the vibration of symmetrical valence stretching P-O(H) of the structuraL HPO_4^{2-} group. If the gypsum-brushite mixture is homogeneous, it is possible to relate it to the height of this absorption band and the amount of brushite introduced (Aslanian et al., 1980).

In a solid solution with 5 wt% HPO_4^{2-} only the band at 837 cm^{-1} is present (see Fig. 12), representing the syncrystallized phosphate ion HPO_4^{2-}, while the band at 872 cm^{-1} appears at 10 wt% HPO_4^{2-} in the solid solution corresponds to the demixing of the solid solution gypsum (SO_4^{2-}, HPO_4^{2-}) into two gypsum phases (HPO_4^{2-} syncrystallized) and ardealite ($Ca(SO_4)_{1-x}(HPO_4)_x2H_2O$). At 40–50 wt% HPO_4^{2-} only the 872 cm^{-1} band remains which corresponds to the HPO_4^{2-} ion of ardealite.

The IR studies of gypsum samples containing varying amounts of HPO_4^{2-} showed that the primary absorption band of syncrystallized HPO_4^{2-} ions, found at 836 cm^{-1}, increased in intensity until it reached a

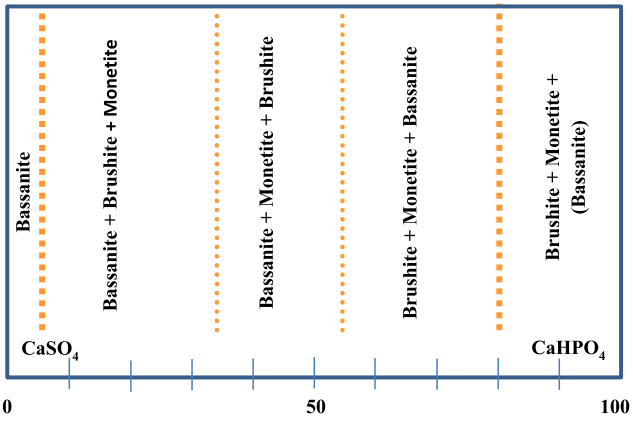

Fig. 10. Phases present in the $CaSO_4.2H_2O$ - $CaHPO_4.2H_2O$ system heated to 150 °C determined by XRD.

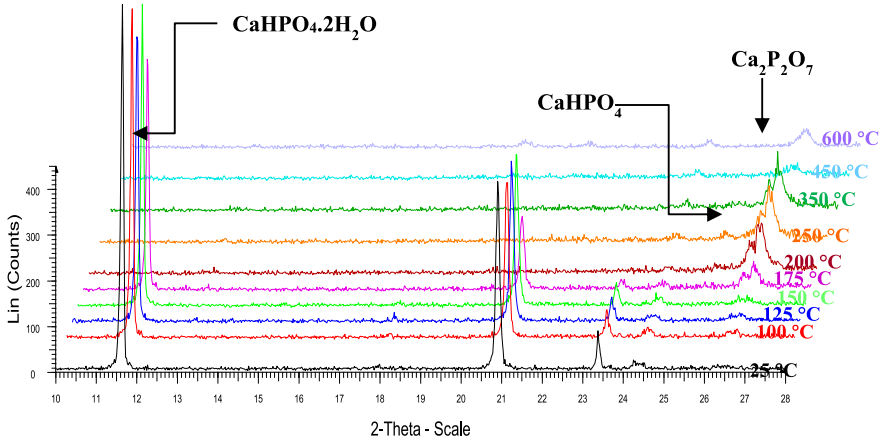

Fig. 9. A series of XRD patterns taken during the calcination of brushite.

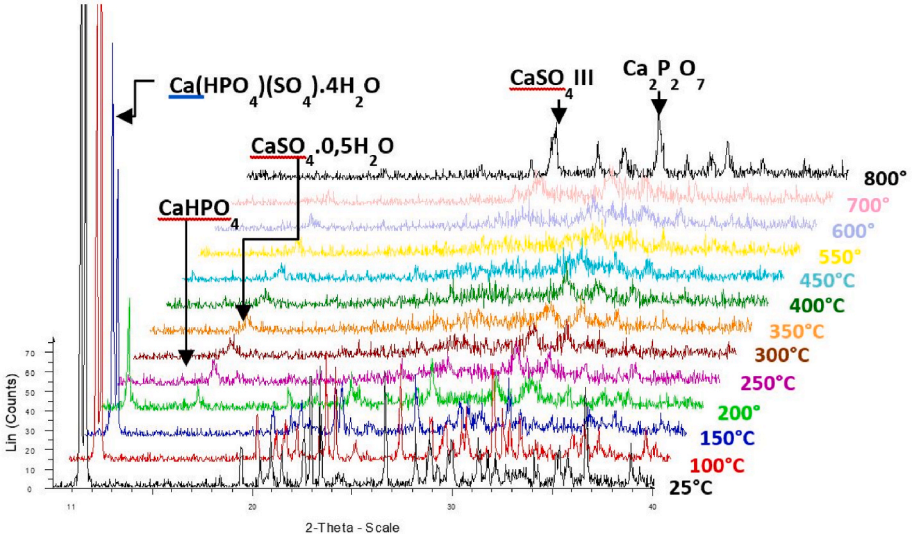

Fig. 11. A series of XRD patterns taken during the calcination of ardealite.

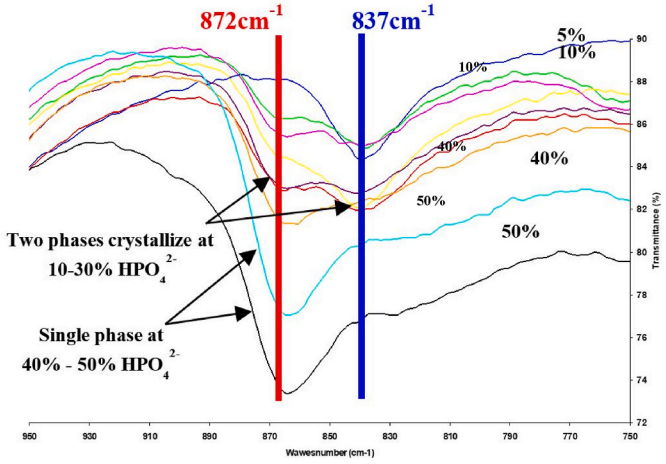

Fig. 12. Infrared absorption spectrum of a solid solution as a function of the contents by weight of $CaHPO_4 2H_2O/CaSO_4 2HO + CaHPO_4 2H_2O$) = 5, 10, 12, 13, 15, 20, 30, 40 and 50.

Table 3
Summary of the waves corresponding to the absorption bands of HPO_4^{2-} observed on the infrared spectra of solid solution gypsum and of the gypsum-brushite mixture.

	Characteristic bands of HPO_4^{2-} wavelengths (cm^{-1})			
HPO_4^{2-} (Brushite)	1650	986	872	524
HPO_4^{2-} syn-crystallized	1017		836	

P/S ratio of approximately 0.1111 (see Fig. 13). However, as the proportion of inserted phosphate ions continues to rise, the intensity of the absorption band decreases and eventually disappears when the P/S ratio reaches 0.4287. Simultaneously, the characteristic absorption band of ardealite appears for P/S = 0.1111 at 864 cm^{-1}. The intensity of this band is raised with an increase of the P_2O_5 percentage and gradually shifts to higher wavelengths. For P/S ≅ 4, the absorption band was found at 870 cm^{-1}, and it shifts to 872 cm^{-1} for pure brushite. Therefore, it was impossible for us to establish a limit between the passage from the ardealite phase to the brushite phase using this analysis technique. In this spectral range, Aslanian et al. (1980) had only identified two absorption bands: the band at 850 cm^{-1} which appeared for a P/S = 0.080 but was not attributed, and the 872 cm^{-1} band identified for a P/S ratio above 0.25. Similarly, Rinaudo and Abbona (1988) also found that the spectrum of synthetic ardealite is different from that of a mixture of gypsum and brushite. However, they have not mentioned the presence of the 864 cm^{-1} absorption band. It would be interesting to analyse in more detail the part where $HPO_4^{2-} > 96\%$. Contrary to the $HPO_4^{2-} < 3\%$ area, the characteristic absorption bands of HPO_4^{2-} (SO_4^{2-} ions substituted by HPO_4^{2-}) in the gypsum phase that can be observed relatively easily, it seems difficult to determine the absorption bands relative to SO_4^{2-} ions in the brushite lattice, considering the observations made above. We were indeed not able to observe a new absorption band but only a shift of the band located at 872 cm^{-1} relative to the brushite.

In the spectral range from 500 to 700 cm^{-1}, it was observed that as the amount of P_2O_5 increased, the absorption band characteristic of syncrystallized HPO_4^{2-} ions located at 527 cm^{-1} intensified and shifted to 517 cm^{-1}, a band attributed to pure brushite (see Fig. 13). Moreover, for P/S = 4, the bands at 668 and 597 cm^{-1} disappeared and a new absorption band at 576 cm^{-1} could be observed.

The solid solution containing HPO_4^{2-} syncrystallized ions was characterized with respect to the gypsum-brushite mechanical mixture by the presence of two absorption bands: 1017 cm^{-1} corresponding to the ν_3 vibration of asymmetric valence stretching P-O(H) of the structural group $(PO_4)^{3-}$ and 837 cm^{-1} vibration linked to the structural group HPO_4^{2-}, the latter being on average twice as important. It can be noted that there is a very good correlation between the quantity of syncrystallized HPO_4^{2-} ions introduced into the solid solution gypsum and the height of the peak of the absorption band (Fig. 14). If the gypsum-brushite mixture is homogeneous, it is possible to relate the height of this absorption band to the amount of brushite introduced (see Fig. 14) (Aslanian et al., 1980; Bard and Bilal, 2011; Bilal et al., 2014; Bourgier, 2007; Dumitras et al., 2004, 2011; Laborde, 2002; Marincea et al., 2004).

During the dehydration of synthetic PG, the transformation of anhydrite III to anhydrite II occurs at higher temperatures than for pure gypsum. The brushite present in the mixture is transformed at 150 °C into two phases (Fig. 15): 24% brushite and 76% monetite (semi-hydrated phase). On the DSC curve an endothermic effect can be observed at 156°C and 199°C corresponding to the departure of molecular water. The work on synthetic brushite by C. Rinaudo and Abbona (1988); Sivakumar et al. (1998) agree with our observations on this double endothermic effect.

The mass loss in the first step is 4.11% corresponding to weakly bound molecular water and the second mass loss is 16.42%, or 20.53%

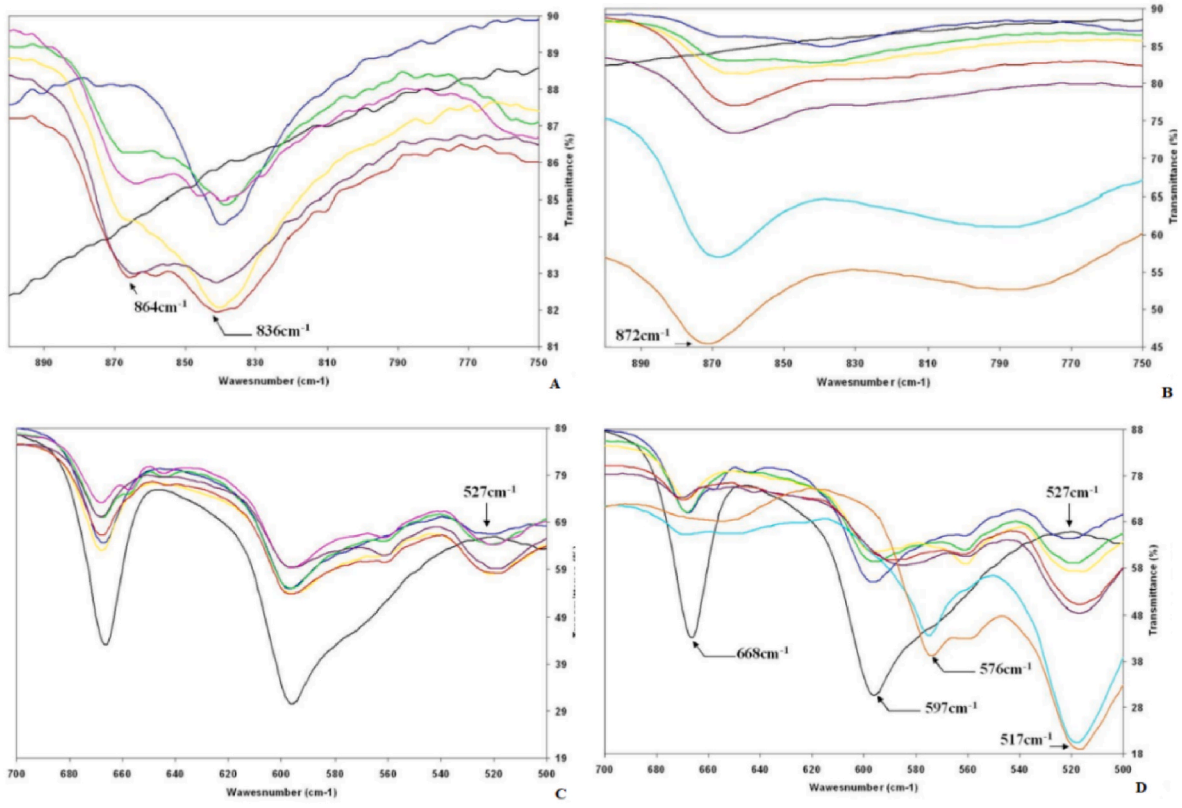

Fig. 13. Infrared spectra of gypsum samples containing 0.00% < HPO_4^{2-} <100.00% A and B) 700-950 cm^{-1} C and D) 500-700 cm^{-1}. $CaSO_4.2H_2O$, P/S = 0.0526, 0.1111, 0.1364, 0.1494, 0.1522, 0.2500 (Figs. A and C). $CaSO_4.2H_2O$, P/S = 0.1111, 0.2500, 0.4287, 0.6666, 1.0000, 1.5000, 4.0000, $CaHPO_4.2H_2O$ (Figs. B and D).

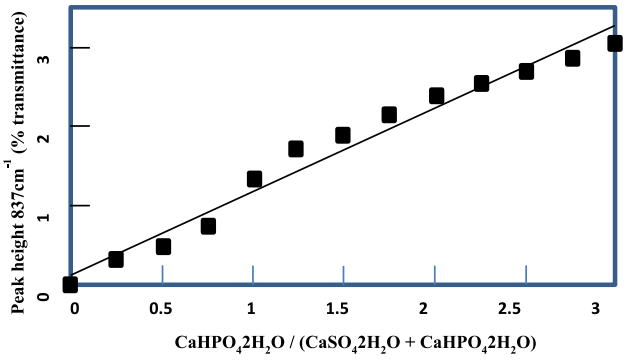

Fig. 14. Correlation between the height of the 837 cm^{-1} absorption band and the content of HPO_4^{2-} syncrystallized ions.

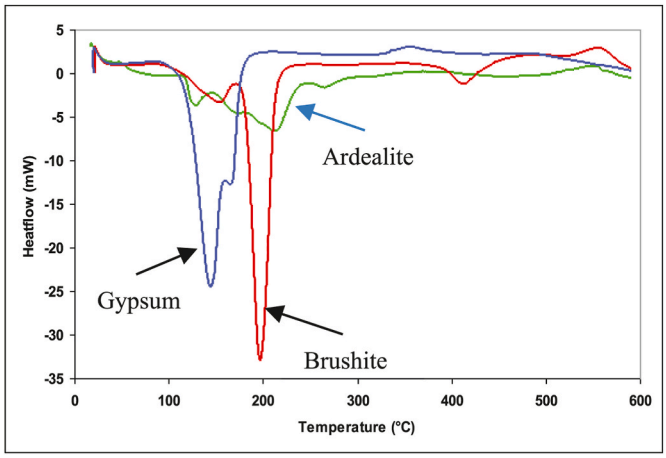

Fig. 15. Dehydration of the pure gypsum (blue), brushite (red) and ardealite (green) phases. (For interpretation of the references to colour in this figure legend, the reader is referred to the Web version of this article.)

of the total cumulative mass loss. The third mass loss of 4.81% at 415 °C corresponds to the disappearance of monetite and the formation of $Ca_2P_2O_7$ corresponding to the exothermic peak of the DSC curve (Fig. 16).

The dehydration of ardealite occurs in several stages with endothermic peaks at 135 °C, 165 °C, 190 °C and 215 °C (Rinaudo and Abbona, 1988) and results in a total mass loss of about 20%.

4. PG circular economy considerations

The extractive nature of mining does not enable the raw material industry to become fully circular. In other words, the nature of mining will unavoidably make it environmentally disruptive (Schoenberger, 2016; Zhao et al., 2012). There is still plenty of room for the mining industry (de la Torre de Palacios and Espí Rodríguez, 2022; Gorman and Dzombak, 2018; Laurence, 2011; Littleboy et al., 2019; Whitmore, 2006), and also the phosphate ore mining industry (Geissler et al., 2018) to become more sustainable though. The extractive industries surely are part of the economy, providing the raw materials for all other activities, and they will therefore also be a part of any envisioned circular economy (Lèbre et al., 2017a; Singh et al., 2020). Circular economy considerations in mining usually focus on minimizing the environmental impact during raw material extraction (Input in Fig. 17) and minimizing the quantity as well as the environmental impact of the produced waste (Output in Fig. 17) (Cimprich et al., 2022; Gedam et al., 2021; Luthra et al., 2022; Tayebi-Khorami et al., 2019). There is a fine, and we like to

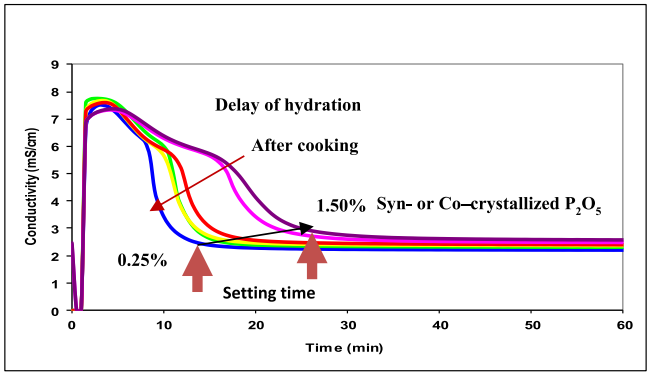

Fig. 16. Conductometric curves and stabilization time of conductivity (setting time) of synthetic PG with different P_2O_5 contents and hydration of synthetic PG cooking.

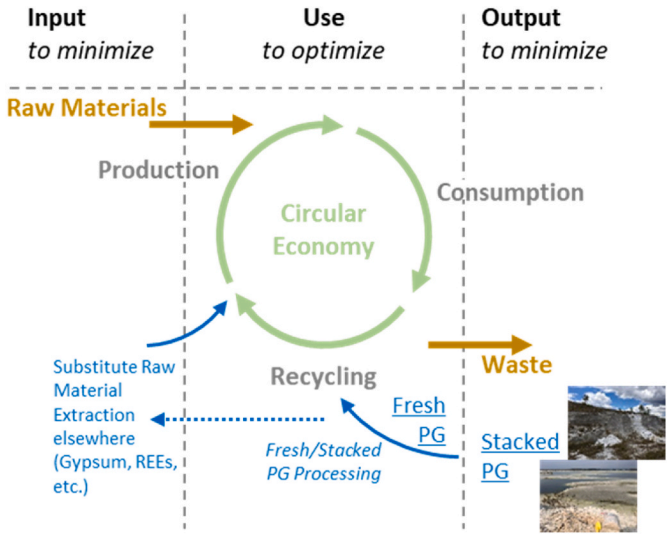

Fig. 17. Circular economy considerations for PG.

think permeable, line between what is a waste and what might be a resource (Lèbre et al., 2017b). This is even more true for naturally occurring radioactive material (NORM) or technologically enhanced NORM (TENORM) such as PG that are often overlooked in circular economy considerations (Tsioka and Voudrias, 2020; Turcanu et al., 2022). Fig. 17 provides a simplified illustration of our understanding of the circular economy with considerations for fresh- and stacked PG. Specifically, we believe that fresh PG should ideally not be considered a waste but be processed and thus stay within the circular economy consisting of production, consumption, and recycling in Fig. 17 (Xu et al., 2019). The considerable quantities of stacked PG (3–8 billion t worldwide) can also be processed and thus added to the circular economy, minimizing raw material extraction, for instance for natural gypsum and rare earths, elsewhere.

Policies to support the re-use of PG as illustrated in Fig. 17 are already underway (Cui et al., 2022) and we sincerely hope that this review will add knowledge that can further foster the utilization of fresh and stacked PG as a valuable secondary resource. This practice would not only reduce environmental risks associated with storing PG but also free a considerable amount of land that can then be used for other purposes.

This work allowed us to compare a relatively large number of PG samples with one another and learn about the different national practices and regulations in the process. It is challenging to draw generally applicable conclusions from such a large dataset. We are confident to share though that directly marketable PG needs to fulfill strict specification that usually depend on its free moisture content, total P_2O_5 content, soluble and insoluble P_2O_5 content, the PG insoluble F and soluble F content, pH, the particle size, morphology, texture, and radioactivity index. The chapters of this review were in fact designed accordingly to add our experience about PG analysis and processing. This experience also showed that washing with diluted sulfuric acid, morphological and chemical characterization can be simple but powerful methods to identify marketable PG.

Table 4
Specification of PG for use in the plaster industry.

Free Moisture %	If possible <15
Total P_2O_5%	<1
Insoluble P_2O_5%	<0.6
Soluble P_2O_5%	<0.05
Co-crystallized P_2O_5%	<0,5
Total F	<1
Insoluble F%	<0.6
Co-crystallized F	<0,15
Soluble F%	<0.05
Na_2O %	<0,5
MgO %	<0,6
Chloride	<0,01
pH	5< pH < 8
SiO_2 (quartz & non soluble in HCl acid)	<1,25%
Particle Size: d50	50 μm < d 50 < 100 μm
No needles, no spherical shapes	
RadioactivityIndex I = Ra/300+Th/200+K/3000	Index for final product <1
Additives	None which can penalize setting times
Size specification for shipping	Pellets 20/30 mm or <70 mm
Size specification for utilization	Mixed with clinker then ground

Table 4 provides an example of the PG specifications required for the plaster industry that we consider to be one of the most important takers of fresh and stacked PG worldwide. In this context, it is noteworthy that in case of fresh PG changes in the current phosphoric acid production processes (sulfuric acid use, the temperature of the reaction, the particle size of the phosphate rock and a mixture of different types of magmatic and sedimentary phosphate rock to influence the morphology and texture of the PG) can have significant effects on the resulting PG.

As of now the phosphate fertilizer industry designs the phosphoric acid production processes with the aim of producing the best fertilizers (as they should). Not at all considering or having to consider the quality of the produced PG, can however, result in PG that is a particularly hard sell. We sincerely hope that this *one-product-thinking* will change to a *multi-product-thinking* as part of which the quality of both phosphoric acid and PG are considered in the process designs, so that both can later be sold at ease.

5. Conclusions and outlook

This critical review summarized over 25 years of work on PG utilization at EMSE. PG samples from more than 65 storage sides were considered and novel conclusions on s-PG and m-PG, as well as how the processing parameters of these PGs define the PG composition are provided. Besides, the critical review puts an emphasis on providing useful observation for PG analysis and introduces an important way to group PG samples by its texture and morphology that is particularly relevant if PG is investigated for potential use as a construction material. Although a relatively large set of samples was used in this critical review tracing the PG back to the raw material utilized was sometimes challenging as industrial samples were used and the companies providing them had an interest to not fully disclose processing as well as mixing parameters. Future studies should aim for more transparency and also more consistency with regards to sample analysis and comparison so that further conclusions, relevant for the utilization of PG can be drawn. Recycling of

PG is an extremely active topic and we provided novel, higher-level analysis of the role of fresh and stacked PG in an envisioned circular economy.

Authors statement

Conceptualization, Methodology, Writing-Reviewing and Editing: EB; Writing-Reviewing and Editing: HB, NH; Reviewing and Editing: VB, HM, DGD, FB, ML, JPC, BG, ELI, MB, MAI, SM, ME, BL, RRD, JDR, YC, VC, HR, HS, RB, CRC and JMN. All authors have read and agreed to the published version of the manuscript.

Funding

French National Research Agency (ANR), Ecole Nationale Supérieure des Mines de Saint-Etienne, Lafarge Division Plaster, OCP Group, Technology Agency of the Czech Republic (TA CR) [Grant Number: TH79020003] and German Federal Ministry of Education and Research [Project Number: 033RU020A] support for this project is offered under the coordination of the ERA-MIN3 action, which has received funding from the European Union under the Horizon 2020 Program [European Commission Grant Agreement No. 101003575]. Besides, this work also received support by: the Ministry of Education, Youth and Sport of the Czech Republic (8J22AT005), the Austrian Federal Ministry of Education, Science and Research (BMBWF) through Austria's Agency for Education and Internationalization (OeAD) [Grant Number: Africa UniNet P006 and P058 as well as WTZ CZ 14/2022, HR 09/2022 and TW 01/2021], the German Federal Ministry of Education and Research funding under Bridge2ERA2021 [Grant No. 100579052] and the Spanish Ministry of Economy and Competitiveness through the project VALOREY [MINECO; RTI 2018-101276-J-I00]. C.R. Cánovas further thanks the Spanish Ministry of Science and Innovation for the Postdoctoral Fellowship granted under application reference RYC2019-027949-I.

Declaration of competing interest

The authors declare that they have no known competing financial interests or personal relationships that could have appeared to influence the work reported in this paper.

Data availability

Data will be made available on request.

References

Aagli, A., Tamer, N., Atbir, A., et al., 2005. Conversion of phosphogypsum to potassium sulfate. J Therm Anal Calorim 82, 395–399. https://doi.org/10.1007/s10973-005-0908-y.

Abbes, N., Bilal, E., Hermann, L., Steiner, G., Haneklaus, N., 2020. Thermal Beneficiation of Sra Oertane (Tunisia) Low-Grade Phosphate Rock. Minerals 10 (11), 937. https://doi.org/10.3390/min10110937.

Abdelouahhab, M., Manar, S., Benhida, R., 2022. Optimization and evaluation of the effect of impurities on phosphoric acid process performance using design of experiments. Results Eng 15, 100501. https://doi.org/10.1016/j.rineng.2022.100501.

Abouzeid, A.Z.M., 2008. Physical and thermal treatment of phosphate ores - an overview. Int. J. Miner. Process. 85, 59–84. https://doi.org/10.1016/j.minpro.2007.09.001.

Abu-Eishah, S.I., Abu-Jabal, N.M., 2001. Parametric study on the production of phosphoric acid by the dihydrate process. Chem. Eng. J. 81, 231–250.

Abu-Eishah, S.I., Bani-Kananeh, A.A., Allawzi, M.A., 2000. K2SO4 production via the double decomposition reaction of KCl and phosphogypsum. Chem. Eng. J. 76, 197–207. https://doi.org/10.1016/S1385-8947(99)00158-8.

Adeoye, C., Gupta, J., Demers, N., Adhikari, A., 2021. Variations of radon and airborne particulate matter near three large phosphogypsum stacks in Florida. Environ. Monit. Assess. 193, 1–13. https://doi.org/10.1007/s10661-021-09054-6.

Akfas, F., Elghali, A., Louis, J., Parat, F., Muñoz, M., 2023. Geochemical and mineralogical characterization of phosphogypsum and leaching tests for the prediction of the mobility of trace elements. Environ. Sci. Pollut. Res. https://doi.org/10.1007/s11356-023-25357-2.

Al-Hwaiti, M.S., Ranville, J.F., Ross, P.E., 2010. Bioavailability and mobility of trace metals in phosphogypsum from Aqaba and Eshidiya, Jordan. Chem. Erde 70, 283–291. https://doi.org/10.1016/j.chemer.2010.03.001.

Al-Masri, M.S., Amin, Y., Ibrahim, S., Al-Bich, F., 2004. Distribution of some trace metals in Syrian phosphogypsum. Appl. Geochem. 19, 747–753. https://doi.org/10.1016/J.APGEOCHEM.2003.09.014.

Al Khaledi, N., Taha, M., Hussein, A., Hussein, E., El Yahyaoui, A., Haneklaus, N., 2019. Direct leaching of rare earth elements and uranium from phosphate rocks. In: IOP Conference Series: Materials Science and Engineering. https://doi.org/10.1088/1757-899X/479/1/012065.

Aoun, M., Arnaudguilhem, C., El Samad, O., Khozam, R.B., Lobinski, R., 2015. Impact of a phosphate fertilizer plant on the contamination of marine biota by heavy elements. Environ. Sci. Pollut. Res. 22, 14940–14949. https://doi.org/10.1007/s11356-015-4691-4.

Arhouni, F.E., Hakkar, M., Mahrou, A., Belahbib, L., Mazouz, H., Haneklaus, N., Pavón, S., Bertau, M., Boukhair, A., Ouakkas, S., Abdo, M.A.S., Benjelloun, M., 2022. Better filterability and reduced radioactivity of phosphogypsum during phosphoric acid production in Morocco using a fly ash waste and pure silica additive. J. Radioanal. Nucl. Chem. 331, 1609–1617. https://doi.org/10.1007/s10967-022-08235-y.

Aslanian, S., Stoilova, D., Petrova, R., 1980. Isodimorphe Substitution im CaSO4–CaHPO4–H2O-System. Z. Anorg. Allg. Chem. 465, 209–220. https://doi.org/10.1002/zaac.19804650125.

Asr, E.T., Kakaie, R., Ataei, M., Tavakoli Mohammadi, M.R., 2019. A review of studies on sustainable development in mining life cycle. J. Clean. Prod. 229, 213–231. https://doi.org/10.1016/j.jclepro.2019.05.029.

Balaram, V., 2019. Rare earth elements: a review of applications, occurrence, exploration, analysis, recycling, and environmental impact. Geosci. Front. 10, 1285–1303. https://doi.org/10.1016/j.gsf.2018.12.005.

Balenzano, F., Dell'Anna, L., DI-Pierro, M., Fiore, S., 1984. Ardealite, CaHPO4CaSO4• 4H2O: a new occurrence and new data. Neues Jahrbuch Mineral. Monatsh. 461–467.

Banihashemi, S.R., Taheri, B., Razavian, S.M., Soltani, F., 2021. Nitrophosphate solution purification by calcium precipitation as gypsum. Jom 73, 27–31. https://doi.org/10.1007/s11837-020-04374-3.

Bard, F., Bilal, E., 2011. Semi-batch precipitation of calcium sulfate dihydrate from calcite and sulfuric acid. Carpathian J. earth Environ. Sci. 6, 241–250.

Becker, P., others, 1989. Phosphates and Phosphoric Acid: Raw Materials, Technology, and Economics of the Wet Process. Revised and Expanded. Marcel Dekker, Inc.

Belahbib, L., Arhouni, F.E., Boukhair, A., Essadaoui, A., Ouakkas, S., Hakkar, M., Abdo, M.A.S., Benjelloun, M., Bitar, A., Nourreddine, A., 2021. Impact of phosphate industry on natural radioactivity in sediment, seawater, and coastal marine fauna of El jadida province, Morocco. J. Hazardous, Toxic, Radioact. Waste 25. https://doi.org/10.1061/(asce)hz.2153-5515.0000563.

Beltrami, D., Cote, G., Mokhtari, H., Courtaud, B., Moyer, B.A., Chagnes, A., 2014. Recovery of uranium from wet process phosphoric acid by solvent extraction. Chem. Rev. 114, 12002–12023. https://doi.org/10.1021/cr5001546.

Ben Salem, Z., Ayadi, H., 2017. First investigation of trace metal distribution in surface seawater and copepods of the south coast of Sfax (Tunisia). Environ. Sci. Pollut. Res. 24, 19662–19670. https://doi.org/10.1007/s11356-017-9536-x.

Berry, E.E., Baddiel, C.B., 1967. The infra-red spectrum of dicalcium phosphate dihydrate (brushite). Spectrochim. Acta Part A Mol. Spectrosc. 23, 2089–2097. https://doi.org/10.1016/0584-8539(67)80097-7.

Bilal, E., Bounakhla, M., Benmansour, Mello, 2010. Characterization of Brazilian phosphogypsum. Rom. J. Miner. Deposits 84, 41–44.

Bilal, E., Bourgier, V., Laborde, M., Caspar, J.P., Guilhot, B., Iatan, L., Doumas, M., Bounakhla, M., Dumitras, D.G., I, M.A., M, S., 2014. Phosphogypsum waste or by product. In: Colloque International E3D, Eau, Déchets, Développement Durable. Ales, France.

Bilal, E., Caspar, J.P., 2004. Phosphogypsum Recycling. Internal Report of the Tata Chemical Meeting (Calcutta, India).

Bituh, T., Vučić, Z., Marović, G., Prlić, I., 2013. A new approach to determine the phosphogypsum spread from the deposition site into the environment. J. Hazard Mater. 261, 584–592. https://doi.org/10.1016/j.jhazmat.2013.08.012.

Borilo, A., Skwarzec, B., Olszewski, G., 2012. The radiochemical contamination (210Po and 238U) of zone around phosphogypsum waste heap in Wiślinka (northern Poland). J. Environ. Sci. Heal. Part A2 47, 675–687. https://doi.org/10.1080/10934529.2012.660052.

Bouargane, B., Laaboubi, K., Ghali, M., Bahcine, B., Ali, B., 2023. Effective and innovative procedures to use phosphogypsum waste in different application domains : review of the environmental , economic challenges and life cycle assessment. J. Mater. Cycles Waste Manag. https://doi.org/10.1007/s10163-023-01617-8.

Boudaya, L., Mosbahi, N., Dauvin, J.C., Neifar, L., 2019. Structure of the benthic macrofauna of an anthropogenic influenced area: skhira bay (gulf of gabès, central mediterranean sea). Environ. Sci. Pollut. Res. 26, 13522–13538. https://doi.org/10.1007/s11356-019-04809-8.

Bourgier, V., 2007. Influence des ions monohydrogénophosphates et fluorophosphates sur les propriétés des phosphogypses et la réactivité des phosphoplâtres. Ecole Nationale Supérieure des Mines de Saint-Étienne.

Burnett, W.C., Elzerman, A.W., 2001. Nuclide migration and the environmental radiochemistry of Florida phosphogypsum. J. Environ. Radioact. 54, 27–51. https://doi.org/10.1016/S0265-931X(00)00164-8.

Burnett, W.C., Schultz, M.K., Hull, C.D., 1996. Radionuclide flow during the conversion of phosphogypsum to ammonium sulfate. J. Environ. Radioact. 32, 33–51. https://doi.org/10.1016/0265-931X(95)00078-O.

Cai, Q., Jiang, J., Ma, B., Shao, Z., Hu, Y., Qian, B., Wang, L., 2021. Efficient removal of phosphate impurities in waste phosphogypsum for the production of cement. Sci. Total Environ. 780, 146600 https://doi.org/10.1016/j.scitotenv.2021.146600.
Calderón-Morales, B.R.S., García-Martínez, A., Pineda, P., García-Tenório, R., 2021. Valorization of phosphogypsum in cement-based materials: limits and potential in eco-efficient construction. J. Build. Eng. 44 https://doi.org/10.1016/j.jobe.2021.102506.
Campos, M.P., Costa, L.J.P., Nisti, M.B., Mazzilli, B.P., 2017. Phosphogypsum recycling in the building materials industry: assessment of the radon exhalation rate. J. Environ. Radioact. 172, 232–236. https://doi.org/10.1016/j.jenvrad.2017.04.002.
Cánovas, C.R., Chapron, S., Arrachart, G., Pellet-Rostaing, S., 2019. Leaching of rare earth elements (REEs) and impurities from phosphogypsum: a preliminary insight for further recovery of critical raw materials. J. Clean. Prod. 219, 225–235. https://doi.org/10.1016/j.jclepro.2019.02.104.
Cánovas, C.R., Macías, F., Pérez-López, R., Basallote, M.D., Millán-Becerro, R., 2018. Valorization of wastes from the fertilizer industry: current status and future trends. J. Clean. Prod. 174, 678–690. https://doi.org/10.1016/j.jclepro.2017.10.293.
Cánovas, C.R., Pérez-López, R., Macías, F., Chapron, S., Nieto, J.M., Pellet-Rostaing, S., 2016. Exploration of fertilizer industry wastes as potential source of critical raw materials. J. Clean. Prod. 1–9. https://doi.org/10.1016/j.jclepro.2016.12.083.
Cao, W., Yi, W., Li, J., Peng, J., Yin, S., 2021. A facile approach for large-scale recovery of phosphogypsum: an insight from its performance. Construct. Build. Mater. 309, 125190 https://doi.org/10.1016/j.conbuildmat.2021.125190.
Cao, W., Yi, W., Peng, J., Li, J., Yin, S., 2022. Recycling of phosphogypsum to prepare gypsum plaster: effect of calcination temperature. J. Build. Eng. 45, 103511 https://doi.org/10.1016/j.jobe.2021.103511.
Cao, Y., Cui, Y., Yu, X., Li, T., Chang, I.S., Wu, J., 2021. Bibliometric analysis of phosphogypsum research from 1990 to 2020 based on literatures and patents. Environ. Sci. Pollut. Res. 28, 66845–66857. https://doi.org/10.1007/s11356-021-15237-y.
Cárdenas-Escudero, C., Morales-Florez, V., Pérez-López, R., Santos, A., Esquivias, L., 2011. Procedure to use phosphogypsum industrial waste for mineral CO 2 sequestration. J. Hazard Mater. 196, 431–435. https://doi.org/10.1016/j.jhazmat.2011.09.039.
Chang, W.F., Mantell, M.I., 1990. Engineering Properties and Construction Applications of Phosphogypsum. University of Miami, Phosphate Research Institute, Florida Institute of Phosphate Research.
Chen, M., Graedel, T.E., 2015. The potential for mining trace elements from phosphate rock. J. Clean. Prod. 91, 337–346. https://doi.org/10.1016/j.jclepro.2014.12.042.
Chernysh, Y., Yakhnenko, O., Chubur, V., Roubík, H., 2021. Phosphogypsum recycling: a review of environmental issues, current trends, and prospects. Appl. Sci. 11, 1–22. https://doi.org/10.3390/app11041575.
Choura, M., 2007. Short and Medium Action Program III-Tunisia: Environmental Evaluation of the Treatment of Phosphate in the South Coastal Zone of Sfax. Municipally of Sfax.
Cimprich, A., Young, S.B., Schrijvers, D., Ku, A.Y., Hagelüken, C., Christmann, P., Eggert, R., Habib, K., Hirohata, A., Hurd, A.J., Lee, M.H., Peck, D., Petavratzi, E., Tercero Espinoza, L.A., Wäger, P., Hool, A., 2022. The role of industrial actors in the circular economy for critical raw materials: a framework with case studies across a range of industries. Miner. Econ. https://doi.org/10.1007/s13563-022-00304-8.
Cole, W.F., Lancucki, C.J., 1974. A refinement of the crystal structure of gypsum CaSO4. 2H2O. Acta Crystallogr. Sect. B Struct. Crystallogr. Cryst. Chem. 30, 921–929.
Corona, B., Shen, L., Reike, D., Rosales Carreón, J., Worrell, E., 2019. Towards sustainable development through the circular economy—a review and critical assessment on current circularity metrics. Resour. Conserv. Recycl. 151, 104498 https://doi.org/10.1016/j.resconrec.2019.104498.
Cossa, D., Elbaz-Poulichet, F., Nieto, J.M., 2001. Mercury in the tinto-odiel estuarine system "gulf of cadiz, Spain": sources and dispersion. Aquat. Geochem. 7, 1–12. https://doi.org/10.1023/A:1011392817453.
Cui, Y., Chang, I.S., Yang, S., Yu, X., Cao, Y., Wu, J., 2022. A novel dynamic business model to quantify the effects of policy intervention on solid waste recycling industry: a case study on phosphogypsum recycling in Yichang, China. J. Clean. Prod. 355, 131779 https://doi.org/10.1016/j.jclepro.2022.131779.
Curry, N.A., Jones, D.W., 1971. Crystal structure of brushite, calcium hydrogen orthophosphate dihydrate: a neutron-diffraction investigation. J. Chem. Soc. A Inorganic, Phys. Theor. 3725–3729.
Da Silva, G.A., Kulay, L.A., 2005. Environmental performance comparison of wet and thermal routes for phosphate fertilizer production using LCA - a Brazilian experience. J. Clean. Prod. 13, 1321–1325. https://doi.org/10.1016/j.jclepro.2005.05.004.
de la Torre de Palacios, L., Espí Rodríguez, J.A., 2022. In mining, not everything is a circular economy: case studies from recent mining projects in Iberia. Res. Pol. 78 https://doi.org/10.1016/j.resourpol.2022.102798.
De Vreugd, C.H., Witkamp, G.J., Van Rosmalen, G.M., 1994. Growth of gypsum III. Influence and incorporation of lanthanide and chromium ions. J. Cryst. Growth 144, 70–78.
Diwa, R.R., Tabora, E.U., Palattao, B.L., Haneklaus, N.H., Vargas, E.P., Reyes, R.Y., Ramirez, J.D., 2021. Evaluating radiation risks and resource opportunities associated with phosphogypsum in the Philippines. J. Radioanal. Nucl. Chem. https://doi.org/10.1007/s10967-021-08142-8.
Dumitras, D.-G., Marincea, S., Bilal, E., Constantinescu, E., 2011. Infrared Spectroscopy of Ardealite from the "Type Locality" Cioclovina Uscata Cave, Sureanu Mountains (Romania).
Dumitras, D.-G., Marincea, S., Fransolet, A.-M., 2004. Brushite in the bat guano deposit from the "dry" Cioclovina Cave (sureanu Mountains, Romania). Neues Jahrbuch Mineral. Abhand. 180, 45–64. https://doi.org/10.1127/0077-7757/2004/0180-0045.
Dydo, P., Turek, M., Ciba, J., 2003. Scaling analysis of nanofiltration systems fed with saturated calcium sulfate solutions in the presence of carbonate ions. Desalination 159, 245–251. https://doi.org/10.1016/S0011-9164(03)90076-2.
El-Bahi, S.M., Sroor, A., Mohamed, G.Y., El-Gendy, N.S., 2017. Radiological impact of natural radioactivity in Egyptian phosphate rocks, phosphogypsum and phosphate fertilizers. Appl. Radiat. Isot. 123, 121–127. https://doi.org/10.1016/j.apradiso.2017.02.031.
El-Didamony, H., Gado, H.S., Awwad, N.S., Fawzy, M.M., Attallah, M.F., 2013. Treatment of phosphogypsum waste produced from phosphate ore processing. J. Hazard Mater. 244, 596–602. https://doi.org/10.1016/j.jhazmat.2012.10.053. –245.
El Moussaouiti, M., Boistelle, R., Bouhaouss, A., Klein, J.P., 1996. Agglomeration kinetics of calcium sulphate hemihydrate crystals in sulpho-phosphoric solutions. J. Cryst. Growth 169, 118–123. https://doi.org/10.1016/0022-0248(96)00311-9.
El Zrelli, R., Courjault-Radé, P., Rabaoui, L., Castet, S., Michel, S., Bejaoui, N., 2015. Heavy metal contamination and ecological risk assessment in the surface sediments of the coastal area surrounding the industrial complex of Gabes city, Gulf of Gabes, SE Tunisia. Mar. Pollut. Bull. 101, 922–929. https://doi.org/10.1016/j.marpolbul.2015.10.047.
El Zrelli, R., Rabaoui, L., Abda, H., Daghbouj, N., Pérez-López, R., Castet, S., Aigouy, T., Bejaoui, N., Courjault-Radé, P., 2019. Characterization of the role of phosphogypsum foam in the transport of metals and radionuclides in the Southern Mediterranean Sea. J. Hazard Mater. 363, 258–267. https://doi.org/10.1016/j.jhazmat.2018.09.083.
Elkanzi, E.M., Chalabi, M.F., 1991. Kinetics of the conversion of calcium sulfate to ammonium sulfate using ammonium carbonate aqueous solution. Ind. Eng. Chem. Res. 30, 1289–1293. https://doi.org/10.1021/ie00054a032.
Emsbo, P., McLaughlin, P.I., Breit, G.N., du Bray, E.A., Koenig, A.E., 2015. Rare earth elements in sedimentary phosphate deposits: solution to the global REE crisis? Gondwana Res. 27, 776–785. https://doi.org/10.1016/j.gr.2014.10.008.
Fávaro, D., 2005. Distribution of U and Th decay series and rare earth elements in sediments of Santos Basin: Correlation with industrial activities. J Radioanal Nucl Chem 264, 449–455. https://doi.org/10.1007/s10967-005-0736-3.
Fornés, I.V., Vaičiukynienė, D., Nizevičienė, D., Doroševas, V., Michalik, B., 2021. A comparative assessment of the suitability of phosphogypsum from different origins to be utilised as the binding material of construction products. J. Build. Eng. 44 https://doi.org/10.1016/j.jobe.2021.102995.
Freyer, D., Voigt, W., 2003. Crystallization and phase stability of CaSO4 and CaSO4-based salts. Monatshefte fuer Chemie/Chemical Mon 134, 693–719. https://doi.org/10.1007/s00706-003-0590-3.
Fuleihan, N.F., 2012. Phosphogypsum disposal - the pros & cons of wet versus dry stacking. Procedia Eng. 46, 195–205. https://doi.org/10.1016/j.proeng.2012.09.465.
Gabriel, S., Baschwitz, A., Mathonnière, G., Eleouet, T., Fizaine, F., 2013. A critical assessment of global uranium resources, including uranium in phosphate rocks, and the possible impact of uranium shortages on nuclear power fleets. Ann. Nucl. Energy. https://doi.org/10.1016/j.anucene.2013.03.010.
Garrido, F., Illera, V., García-González, M.T., 2005. Effect of the addition of gypsum- and lime-rich industrial by-products on Cd, Cu and Pb availability and leachability in metal-spiked acid soils. Appl. Geochem. 20, 397–408. https://doi.org/10.1016/J.APGEOCHEM.2004.08.001.
Gedam, V.V., Raut, R.D., Lopes de Sousa Jabbour, A.B., Agrawal, N., 2021. Moving the circular economy forward in the mining industry: challenges to closed-loop in an emerging economy. Res. Pol. 74, 102279 https://doi.org/10.1016/j.resourpol.2021.102279.
Geissler, B., Hermann, L., Mew, M.C., Steiner, G., 2018. Striving toward a circular economy for phosphorus: the role of phosphate rock mining. Minerals 8. https://doi.org/10.3390/min8090395.
Geraldo, R.H., Costa, A.R.D., Kanai, J., Silva, J.S., Souza, J.D., Andrade, H.M.C., Gonçalves, J.P., Fontanini, P.S.P., Camarini, G., 2020. Calcination parameters on phosphogypsum waste recycling. Construct. Build. Mater. 256, 119406 https://doi.org/10.1016/j.conbuildmat.2020.119406.
Gioia, F., Mura, G., Viola, A., 1977. Analysis, simulation, and optimization of the hemihydrate process for the production of phosphoric acid from calcareous phosphorites. Ind. Eng. Chem. Process Des. Dev. 16, 390–399.
Gobbitt, J.M., 2012. YARA Hemihydrate (HH) and Hemidihydrate (HDH) processes for phosphoric acid production. Procedia Eng 46, 143–153. https://doi.org/10.1016/j.proeng.2012.09.457.
Gorman, M.R., Dzombak, D.A., 2018. A review of sustainable mining and resource management: transitioning from the life cycle of the mine to the life cycle of the mineral. Resour. Conserv. Recycl. 137, 281–291. https://doi.org/10.1016/j.resconrec.2018.06.001.
Guilhot, B., Gardet, M., Soustelle, M., Caspar, J.P., Viviers, J., Eymery, J.F., 1974. Etude des impuretés en solution solide dans le gypse : cas des phosphogypses. In: Rapport Interne Confidentiel. Ecole Nationale Supérieure des Mines de Saint-Etienne – L.
Guzmán, E., Regil, E., Pacheco-Malagon, G., 1995. Uranium leaching from phosphate rock. J. Radioanal. Nucl. Chem. 201, 313–320. https://doi.org/10.1007/BF02164050.
Habib, K., Wenzel, H., 2014. Exploring rare earths supply constraints for the emerging clean energy technologies and the role of recycling. J. Clean. Prod. 84, 348–359. https://doi.org/10.1016/j.jclepro.2014.04.035.
Hakim, H., 1997. Mode de gestion du phosphogypse dans l'industrie phosphatière.
Hakkar, M., Arhouni, F.E., Mahrou, A., Bilal, E., Bertau, M., Roy, A., Steiner, G., Haneklaus, N., Mazouz, H., Boukhair, A., Benjelloun, M., 2021. Enhancing rare earth

element transfer from phosphate rock to phosphoric acid using an inexpensive fly ash additive. Miner. Eng. 172, 107166 https://doi.org/10.1016/j.mineng.2021.107166.
Hamdona, S.K., Nessim, R.B., Hamza, S.M., 1993. Spontaneous precipitation of calcium sulphate dihydrate in the presence of some metal ions. Desalination 94, 69–80. https://doi.org/10.1016/0011-9164(93)80155-G.
Haneklaus, N., 2021. Unconventional uranium resources from phosphates. Encycl. Nucl. Energy 286–291. https://doi.org/10.1016/B978-0-12-819725-7.00152-5.
Haneklaus, N., Barbossa, S., Basallote, M.D., Bertau, M., Bilal, E., Chajduk, E., Chernysh, Y., Chubur, V., Cruz, J., Dziarczykowski, K., Fröhlich, P., Grosseau, P., Mazouz, H., Kiegiel, K., Nieto, J.M., Pavón, S., Pessanha, S., Pryzowicz, A., Roubík, H., Cánovas, C.R., Schmidt, H., Seeling, R., Zakrzewska-Kołtuniewicz, G., 2022. Closing the upcoming EU gypsum gap with phosphogypsum. Resour. Conserv. Recycl. 182 https://doi.org/10.1016/j.resconrec.2022.106328.
Haneklaus, N., Bayok, A., Fedchenko, V., 2017a. Phosphate rocks and nuclear proliferation. Sci. Global Secur. 25, 143–158. https://doi.org/10.1080/08929882.2017.1394061.
Haneklaus, N., Sun, Y., Bol, R., Lottermoser, B., Schnug, E., 2017b. To extract, or not to extract uranium from phosphate rock, that is the question. Environ. Sci. Technol. 51, 753–754. https://doi.org/10.1021/acs.est.6b05506.
Hanna, A.A., Akarish, A.I.M., Ahmed, S.M., 2009. Phosphogypsum: Part I: mineralogical, thermogravimetric, chemical and infrared characterization. J. Mater. Sci. \& Technol. 15, 431–434.
Hermann, L., Kraus, F., Hermann, R., 2018. Phosphorus processing-potentials for higher efficiency. Sustain 10. https://doi.org/10.3390/su10051482.
Houghtaling, S.V., 1973. DPG-prayon Modern Dihydrate Process. Pap. Present. before Am. Chem. Soc. Div. Fertil. Soil Chem. Chicago, Illinois.
IAEA, 2013. Safety Reports Series No. 78 Radiation Protection and Management of NORM Residues in the Phosphate Industry.
IFA, 2020. Phosphogypsum Leadership Innovation Partnership.
Jansen, M., Waller, A., Verbiest, J., Van Landschoot, R.C., Van Rosmalen, G.M., 1984. Incorporation of phosphoric acid in calcium sulphate hemihydrate from a phosphoric acid process. Ind Cryst 84, 171–176.
Jia, G., Buchetti, M., Conti, D., Magro, L., Mariani, S., 2022. Radioecological studies of the main naturally occurring radionuclides in the area of Gela Phosphate Industry (Italy) through radioanalytical separation and measurement techniques. Appl. Radiat. Isot. 184, 110173 https://doi.org/10.1016/j.apradiso.2022.110173.
Jia, R., Wang, Q., Luo, T., 2021. Reuse of phosphogypsum as hemihydrate gypsum: the negative effect and content control of H3PO4. Resour. Conserv. Recycl. 174, 105830 https://doi.org/10.1016/j.resconrec.2021.105830.
Jyothi, R.K., Thenepalli, T., Ahn, J.W., Parhi, P.K., Chung, K.W., Lee, J.Y., 2020. Review of rare earth elements recovery from secondary resources for clean energy technologies: grand opportunities to create wealth from waste. J. Clean. Prod. 267, 122048 https://doi.org/10.1016/j.jclepro.2020.122048.
Kandil, A.T., Aly, M.M., Moussa, E.M., Kamel, A.M., Gouda, M.M., Kouraim, M.N., 2010. Column leaching of lanthanides from Abu Tartur phosphate ore with kinetic study. J. Rare Earths 28, 576–580. https://doi.org/10.1016/S1002-0721(09)60157-5.
Kim, H., Eggert, G., Carlsen, R.W., B., W. Dixon, B., 2016. Potential uranium supply from phosphoric acid: a U.S. analysis comparing solvent extraction and Ion exchange recovery. Resour. Policy 49, 222–231. https://doi.org/10.1016/j.resourpol.2016.06.004.
Kinnunen, P.H.M., Kaksonen, A.H., 2019. Towards circular economy in mining: opportunities and bottlenecks for tailings valorization. J. Clean. Prod. 228, 153–160. https://doi.org/10.1016/j.jclepro.2019.04.171.
Kirchherr, J., Reike, D., Hekkert, M., 2017. Conceptualizing the circular economy: an analysis of 114 definitions. Resour. Conserv. Recycl. 127, 221–232. https://doi.org/10.1016/j.resconrec.2017.09.005.
Kitchen, D., 2007. Chemistry of by-product gypsum and plaster. I. Identity of an important solid solution impurity. J. Appl. Chem. Biotechnol. 21, 53–55. https://doi.org/10.1002/jctb.5020210205.
Koopman, C., Witkamp, G.J., 2002. Ion exchange extraction during continuous recrystallization of CaSO4 in the phosphoric acid production process: lanthanide extraction efficiency and CaSO4 particle shape. Hydrometallurgy 63, 137–147. https://doi.org/10.1016/S0304-386X(01)00219-5.
Koopman, C., Witkamp, G.J., 2000. Extraction of lanthanides from the phosphoric acid production process to gain a purified gypsum and a valuable lanthanide. Hydrometallurgy 58, 51–60. https://doi.org/10.1016/S0304-386X(00)00127-4.
Kruger, R.-R., Abriel, W., 1991. Growth and structure refinement of CaSeO4.2H2O. Acta Crystallogr. Sect. C 47, 1958–1959.
Kulczycka, J., Kowalski, Z., Smol, M., Wirth, H., 2016. Evaluation of the recovery of rare earth elements (REE) from phosphogypsum waste - case study of the wizów chemical plant (Poland). J. Clean. Prod. 113, 345–354. https://doi.org/10.1016/j.jclepro.2015.11.039.
Kuzmanović, P., Todorović, N., Mrđa, D., Forkapić, S., Petrović, L.F., Miljević, B., Hansman, J., Knežević, J., 2021. The possibility of the phosphogypsum use in the production of brick: radiological and structural characterization. J. Hazard. Mater. 413 https://doi.org/10.1016/j.jhazmat.2021.125343.
Laborde, M., 2002. Caractérisation du phosphogypse. Ecole Nationale Supérieure des Mines de Saint-Étienne.
Lang, Dupont, 1985. Contribution à l'étude du phosphate bicalcique hydraté. Université de Paris.
Laurence, D., 2011. Establishing a sustainable mining operation: an overview. J. Clean. Prod. 19, 278–284. https://doi.org/10.1016/j.jclepro.2010.08.019.
Lèbre, É., Corder, G., Golev, A., 2017a. The role of the mining industry in a circular economy: a framework for resource management at the mine site level. J. Ind. Ecol. 21, 662–672. https://doi.org/10.1111/jiec.12596.
Lèbre, É., Corder, G.D., Golev, A., 2017b. Sustainable practices in the management of mining waste: a focus on the mineral resource. Miner. Eng. 107, 34–42. https://doi.org/10.1016/j.mineng.2016.12.004.
Lehr, J.R., Frazier, A.W., Smith, J.P., 1966. Phosphoric acid impurities, precipitated impurities in wet-process phosphoric acid. J. Agric. Food Chem. 14, 27–33. https://doi.org/10.1021/jf60143a009.
Li, X., Zhang, Q., 2021. Dehydration behaviour and impurity change of phosphogypsum during calcination. Constr. Build. Mater. 311, 125328 https://doi.org/10.1016/j.conbuildmat.2021.125328.
Littleboy, A., Keenan, J., Ordens, C.M., Shaw, A., Tang, R.H., Verrier, B., Vivoda, V., Yahyaei, M., Hodge, R.A., 2019. A sustainable future for mining by 2030? Insights from an expert focus group. Extr. Ind. Soc. 6, 1086–1090. https://doi.org/10.1016/j.exis.2019.11.005.
Liu, S., Fang, P., Ren, J., Li, S., 2020. Application of lime neutralised phosphogypsum in supersulfated cement. J. Clean. Prod. 272, 122660 https://doi.org/10.1016/j.jclepro.2020.122660.
Liu, T., Chen, J., 2021. Extraction and separation of heavy rare earth elements : a review. Sep. Purif. Technol. 276, 119263 https://doi.org/10.1016/j.seppur.2021.119263.
López, L., Castro, L.N., Scasso, R.A., Grancea, L., Tulsidas, H., Haneklaus, N., 2019. Uranium supply potential from phosphate rocks for Argentina's nuclear power fleet. Resour. Policy 62, 397–404. https://doi.org/10.1016/j.resourpol.2019.04.008.
Luthra, S., Mangla, S.K., Sarkis, J., Tseng, M.L., 2022. Resources melioration and the circular economy: sustainability potentials for mineral, mining and extraction sector in emerging economies. Resour. Policy 77, 102652. https://doi.org/10.1016/j.resourpol.2022.102652.
Lütke, S.F., Oliveira, M.L.S., Silva, L.F.O., Cadaval, T.R.S., Dotto, G.L., 2020. Nanominerals assemblages and hazardous elements assessment in phosphogypsum from an abandoned phosphate fertilizer industry. Chemosphere 256, 127138. https://doi.org/10.1016/j.chemosphere.2020.127138.
Lütke, S.F., Oliveira, M.L.S., Waechter, S.R., Silva, L.F.O., Cadaval, T.R.S., Duarte, F.A., Dotto, G.L., 2022. Leaching of rare earth elements from phosphogypsum. Chemosphere 301, 134661. https://doi.org/10.1016/j.chemosphere.2022.134661.
Lysandrou, M., Pashalidis, I., 2008. Uranium chemistry in stack solutions and leachates of phosphogypsum disposed at a coastal area in Cyprus. J. Environ. Radioact. 99, 359–366. https://doi.org/10.1016/j.jenvrad.2007.08.005.
Macías, F., Cánovas, C.R., Cruz-hernández, P., Carrero, S., Asta, M.P., Miguel, J., Pérez-lópez, R., 2017. An anomalous metal-rich phosphogypsum : characterization and classification according to international regulations. J. Hazard. Mater. 331, 99–108. https://doi.org/10.1016/j.jhazmat.2017.02.015.
Mancheri, N.A., Sprecher, B., Bailey, G., Ge, J., Tukker, A., 2019. Resources , Conservation & Recycling E ff ect of Chinese policies on rare earth supply chain resilience. Resour. Conserv. Recycl. 142, 101–112. https://doi.org/10.1016/j.resconrec.2018.11.017.
Manning, D.A.C., 2008. Phosphate minerals, environmental pollution and sustainable agriculture. Elements 4, 105–108. https://doi.org/10.2113/GSELEMENTS.4.2.105.
Marincea, S., Dumitras, D.-G., Diaconu, G., Bilal, E., 2004. Hydroxylapatite, brushite and ardealite in the bat guano deposit from Pestera Mare de la Mereti, Persani Mountains, Romania. Neues Jahrb. für Mineral. - Monatshefte 464–488. https://doi.org/10.1127/0028-3649/2004/2004-0464, 2004.
Martynowicz, E., 1994. Impurity Uptake in Calcium Sulfate during Phosphoric Acid Processing. Delft University of Technology.
Martynowicz, E., Liao, L., Witkamp, G.J., Van Rosmalen, G.M., 1996a. The influence of aluminium fluoride in hemi-dihydrate phosphoric acid processes. Hydrometallurgy 41, 155–170. https://doi.org/10.1016/0304-386X(95)00054-K.
Martynowicz, E., Witkamp, G.J., Van Rosmalen, G.M., 1996b. The effect of aluminium fluoride on the formation of calcium sulfate hydrates. Hydrometallurgy 41, 171–186. https://doi.org/10.1016/0304-386X(95)00066-P.
Mathew, M., Takagi, S., Waerstad, K.R., Frazier, A.W., 1981. The crystal structure of synthetic chukhrovite, Ca4AlSi(SO4)F13 · 12H2O. Am. Mineral. 66, 392–397.
Mittal, A., Rakshit, D., 2020. Utilization of cement rotary kiln waste heat for calcination of phosphogypsum. Therm. Sci. Eng. Prog. 20, 100729 https://doi.org/10.1016/j.tsep.2020.100729.
Mohammed, F., Biswas, W.K., Yao, H., Tadé, M., 2018. Sustainability assessment of symbiotic processes for the reuse of phosphogypsum. J. Clean. Prod. 188, 497–507. https://doi.org/10.1016/j.jclepro.2018.03.309.
Mudd, G.M., 2014. The future of Yellowcake: a global assessment of uranium resources and mining. Sci. Total Environ. 472, 590–607. https://doi.org/10.1016/j.scitotenv.2013.11.070.
Mulopo, J., Omoregbe, D.I., 2012. Phosphogypsum conversion to calcium carbonate and utilization for remediation of acid mine drainage. J. Chem. Eng. Process Technol. 3, 2–7. https://doi.org/10.4172/2157-7048.1000129.
Murat, M., 1982. Sulfates de calcium et matériaux dérivés. Rapport de synthèse sur les méthodes d'analyse (détermination de la composition chimique et minéralogique). Matériaux et Constructions 15, 63–91. https://doi.org/10.1007/BF02473559.
Mwalongo, D.A., Haneklaus, N.H., Lisuma, J.B., Kivevele, T.T., Mtei, K.M., 2022. Uranium in phosphate rocks and mineral fertilizers applied to agricultural soils in East Africa. Environ. Sci. Pollut. Res. https://doi.org/10.1007/s11356-022-24574-5.
Ojeda-Pereira, I., Campos-Medina, F., 2021. International trends in mining tailings publications: a descriptive bibliometric study. Resour. Policy 74. https://doi.org/10.1016/j.resourpol.2021.102272.
Onac, B.P., Breban, R., Kearns, J., Timat, T., 2002. Unusual minerals related to phosphate deposits in Cioclovina Cave, Şureanu Mts. (Romania). Theor. Appl. Karstology 15, 27–34.
Palla, S., Sharma, P., Rao, M.V.R., Ramakrishna, S., Vanguri, S., Mohapatra, B.N., 2022. Solar thermal treatment of phosphogypsum and its impact on the mineralogical

modification for effective utilization in cement production. J. Build. Eng. 51 https://doi.org/10.1016/j.jobe.2022.104218.
Pérez-lópez, R., Macías, F., Ruiz, C., Miguel, A., Pérez-moreno, S.M., 2016. Science of the Total Environment Pollutant fl ows from a phosphogypsum disposal area to an estuarine environment : an insight from geochemical signatures. Sci. Total Environ. 553, 42–51. https://doi.org/10.1016/j.scitotenv.2016.02.070.
Pérez-López, R., Nieto, J.M., de la Rosa, J.D., Bolívar, J.P., 2015. Environmental tracers for elucidating the weathering process in a phosphogypsum disposal site: implications for restoration. J. Hydrol. 529, 1313–1323. https://doi.org/10.1016/j.jhydrol.2015.08.056.
Petrov, I., Šoptrajanov, B., Fuson, N., Lawson, J.R., 1967. Infra-red investigation of dicalcium phosphates. Spectrochim. Acta Part A Mol. Spectrosc. 23, 2637–2646. https://doi.org/10.1016/0584-8539(67)80155-7.
Pliaka, M., Gaidajis, G., 2022. Potential uses of phosphogypsum: a review. J. Environ. Sci. Heal. Part A 1–18. https://doi.org/10.1080/10934529.2022.2105632.
Ptáček, P., 2016. Apatites and their Synthetic Analogues - Synthesis, Structure, Properties and Applications. InTech. https://doi.org/10.5772/59882.
Pufahl, P.K., Groat, L.A., 2017. Sedimentary and igneous phosphate deposits: formation and exploration: an invited paper. Econ. Geol. 112, 483–516. https://doi.org/10.2113/econgeo.112.3.483.
Qamouche, K., Chetaine, A., Elyahyaoui, A., Moussaif, A., Touzani, R., Benkdad, A., Amsil, H., Laraki, K., Marah, H., 2020. Radiological characterization of phosphate rocks, phosphogypsum, phosphoric acid and phosphate fertilizers in Morocco: an assessment of the radiological hazard impact on the environment. Mater. Today Proc. 27, 3234–3242. https://doi.org/10.1016/j.matpr.2020.04.703.
Qin, X., Cao, Y., Guan, H., Hu, Q., Liu, Z., Xu, J., Hu, B., Zhang, Z., Luo, R., 2023. Resource utilization and development of phosphogypsum-based materials in civil engineering. J. Clean. Prod. 387 https://doi.org/10.1016/j.jclepro.2023.135858.
Ramirez, J.D., Diwa, R.R., Palattao, B.L., Haneklaus, N.H., Tabora, E.U., Bautista, A.T., Reyes, R.Y., 2022. Rare earths in Philippine phosphogypsum: use them or lose them. Extr. Ind. Soc. 10, 101082 https://doi.org/10.1016/j.exis.2022.101082.
Rashad, A.M., 2017. Phosphogypsum as a construction material. J. Clean. Prod. 166, 732–743. https://doi.org/10.1016/j.jclepro.2017.08.049.
Rinaudo, C., Abbona, F., 1988. A contribution to the study of the crystal chemistry of calcium sulfate phosphate hydrate. Miner. Petrogr. Acta 31, 95–105.
Rinaudo, C., Abbona, F., 1988. A contribution to the study of the crystal chemistry of calcium sulphate phosphate hydrate. Acta Mineral. Petrol. 95–105.
Rinaudo, C., Lanfranco, A.M., Franchini-Angela, M., 1994. The system CaHPO4·2H2O-CaSO4·2H2O: crystallizations from calcium phosphate solutions in the presence of SO2-4. J. Cryst. Growth 142, 184–192. https://doi.org/10.1016/0022-0248(94)90287-9.
Roode-Gutzmer, Q., Strydom, C., 1999. The Characterization of Phosphogypsum and Gypsum-Brushite Mixtures by X-Ray Diffraction, Thermogravimetric and Differential Scanning Calorimetric Techniques.
Rosales, J., Pérez, S.M., Cabrera, M., Gázquez, M.J., Bolivar, J.P., de Brito, J., Agrela, F., 2020. Treated phosphogypsum as an alternative set regulator and mineral addition in cement production. J. Clean. Prod. 244 https://doi.org/10.1016/j.jclepro.2019.118752.
Roshdy, O.E., Haggag, E.A., Masoud, A.M., Bertau, M., Haneklaus, N., Pavón, S., Hussein, A.E.M., Khawassek, Y.M., Taha, M.H., 2023. Leaching of rare earths from Abu Tartur (Egypt) phosphate rock with phosphoric acid. J. Mater. Cycles Waste Manag. 25, 501–517. https://doi.org/10.1007/s10163-022-01558-8.
Rutherford, P.M., Dudas, M.J., Arocena, J.M., 1996. Heterogeneous distribution of radionuclides, barium and strontium in phosphogypsum by-product. Sci. Total Environ. 180, 201–209. https://doi.org/10.1016/0048-9697(95)04939-8.
Rutherford, P.M., Dudas, M.J., Arocena, J.M., 1995. Radioactivity and elemental composition of phosphogypsum produced from three phosphate rock sources. Waste Manag. Res. 13, 407–423. https://doi.org/10.1177/0734242X9501300502.
Rutherford, P.M., Dudas, M.J., Samek, R.A., 1994. Environmental impacts of phosphogypsum. Sci. Total Environ. 149, 1–38. https://doi.org/10.1016/0048-9697(94)90002-7.
Rychkov, V.N., Kirillov, E.V., Kirillov, S.V., Semenishchev, V.S., Bunkov, G.M., Botalov, M.S., Smyshlyaev, D.V., Malyshev, A.S., 2018. Recovery of rare earth elements from phosphogypsum. J. Clean. Prod. 196, 674–681. https://doi.org/10.1016/j.jclepro.2018.06.114.
Saadaoui, E., Ghazel, N., Ben Romdhane, C., Massoudi, N., 2017. Phosphogypsum: potential uses and problems–a review. Int. J. Environ. Stud. 74, 558–567. https://doi.org/10.1080/00207233.2017.1330582.
Santos, A.J.G., Mazzilli, B.P., Fávaro, D.I.T., Silva, P.S.C., 2006. Partitioning of radionuclides and trace elements in phosphogypsum and its source materials based on sequential extraction methods. J. Environ. Radioact. 87, 52–61. https://doi.org/10.1016/J.JENVRAD.2005.10.008.
Schoenberger, E., 2016. Environmentally sustainable mining: the case of tailings storage facilities. Resour. Policy 49, 119–128. https://doi.org/10.1016/j.resourpol.2016.04.009.
Scholz, R.W., Wellmer, F.W., 2018. Although there is no physical short-term scarcity of phosphorus, its resource efficiency should be improved. J. Ind. Ecol. 00, 1–6. https://doi.org/10.1111/jiec.12750.
Sebbahi, S., Chameikh, M., Sahban, F.F., Jilali, A., Benarafa, L., Belkbir, L., 1997. Thermal behaviour of Moroccan phosphogypsum. Thermochim. Acta 302, 69–75. https://doi.org/10.1016/S0040-6031(97)00159-7.
Secco, M., Lampronti, G.I., Schlegel, M.-C., Maritan, L., Zorzi, F., 2015. Degradation processes of reinforced concretes by combined sulfate–phosphate attack. Cem. Concr. Res. 68, 49–63. https://doi.org/10.1016/j.cemconres.2014.10.023.
Shang, D., Geissler, B., Mew, M., Satalkina, L., Zenk, L., Tulsidas, H., Barker, L., El-Yahyaoui, A., Hussein, A., Taha, M., Zheng, Y., Wang, M., Yao, Y., Liu, X., Deng, H., Zhong, J., Li, Z., Steiner, G., Bertau, M., Haneklaus, N., 2021. Unconventional uranium in China's phosphate rock: review and outlook. Renew. Sustain. Energy Rev. 140, 110740 https://doi.org/10.1016/j.rser.2021.110740.
Silva, L.F.O., Oliveira, M.L.S., Crissien, T.J., Santosh, M., Bolivar, J., Shao, L., Dotto, G.L., Gasparotto, J., Schindler, M., 2022. A review on the environmental impact of phosphogypsum and potential health impacts through the release of nanoparticles. Chemosphere 286, 131513. https://doi.org/10.1016/j.chemosphere.2021.131513.
Singh, M., 2002. Treating waste phosphogypsum for cement and plaster manufacture. Cem. Concr. Res. 32, 1033–1038. https://doi.org/10.1016/S0008-8846(02)00723-8.
Singh, R.K., Kumar, A., Garza-Reyes, J.A., de Sá, M.M., 2020. Managing operations for circular economy in the mining sector: an analysis of barriers intensity. Resour. Policy 69, 101752. https://doi.org/10.1016/j.resourpol.2020.101752.
Sivakumar, G.R., Girija, E.K., Kalkura, S.N., Subramanian, C., 1998. Crystallization and characterization of calcium phosphates: brushite and monetite. Cryst. Res. Technol. 33, 197–205.
Steiner, G., Geissler, B., Haneklaus, N., 2020. Making uranium recovery from phosphates great again? Environ. Sci. Technol. 54, 1287–1289. https://doi.org/10.1021/acs.est.9b07859.
Tayebi-Khorami, M., Edraki, M., Corder, G., Golev, A., 2019. Re-thinking mining waste through an integrative. Minerals 9 (5), 286. https://doi.org/10.3390/min9050286.
Tayibi, H., Choura, M., López, F.A., Alguacil, F.J., López-Delgado, A., 2009. Environmental impact and management of phosphogypsum. J. Environ. Manage. 90, 2377–2386. https://doi.org/10.1016/j.jenvman.2009.03.007.
Tortet, L., Gavarri, J.-R., Nihoul, G., Fulconis, J.M., Rouquerol, F., 1996. Dehydration and electrochemical activity of calcium hydrogenophosphate dihydrate. Eur. J. Solid State Inorg. Chem. 33, 1199–1210.
Trpkovska, M., Šoptrajanov, B., Malkov, P., 1999. FTIR reinvestigation of the spectra of synthetic brushite and its partially deuterated analogues. J. Mol. Struct. 480–481, 661–666. https://doi.org/10.1016/S0022-2860(98)00923-5.
Tsioka, M., Voudrias, E.A., 2020. Comparison of alternative management methods for phosphogypsum waste using life cycle analysis. J. Clean. Prod. 266, 121386 https://doi.org/10.1016/j.jclepro.2020.121386.
Tulsidas, H., Gabriel, S., Kiegiel, K., Haneklaus, N., 2019. Uranium resources in EU phosphate rock imports. Resour. Policy 61, 151–156. https://doi.org/10.1016/j.resourpol.2019.02.012.
Turcanu, C., Perko, T., Muric, M., Popic, J.M., Geysmans, R., Železnik, N., 2022. Societal aspects of NORM: an overlooked research field. J. Environ. Radioact. 244–245. https://doi.org/10.1016/j.jenvrad.2022.106827.
Upadhyay, A., Laing, T., Kumar, V., Dora, M., 2021. Exploring barriers and drivers to the implementation of circular economy practices in the mining industry. Resour. Policy 72, 102037. https://doi.org/10.1016/j.resourpol.2021.102037.
Van Der Sluis, S., Witkamp, G.J., Van Rosmalen, G.M., 1986. Crystallization of calcium sulfate in concentrated phosphoric acid. J. Cryst. Growth 79, 620–629. https://doi.org/10.1016/0022-0248(86)90529-4.
van Selst, R., Penders, L., Bos, W., 1997. Processing and application of phosphoric gypsum. Stud. Environ. Sci. 71, 603–615. https://doi.org/10.1016/S0166-1116(97)80244-0.
Walawalkar, M., Nichol, C.K., Azimi, G., 2016. Process investigation of the acid leaching of rare earth elements from phosphogypsum using HCl, HNO3, and H2SO4. Hydrometallurgy 166, 195–204. https://doi.org/10.1016/j.hydromet.2016.06.008.
Wang, B., Yang, L., Cao, J., 2021a. The influence of impurities on the dehydration and conversion process of calcium sulfate dihydrate to $α$-calcium sulfate hemihydrate in the two-step wet-process phosphoric acid production. ACS Sustain. Chem. Eng. 9, 14365–14374.
Wang, B., Yang, L., Luo, T., Cao, J., 2021b. Study on the kinetics of hydration transformation from hemihydrate phosphogypsum to dihydrate phosphogypsum in simulated wet process phosphoric acid. ACS omega 6, 7342–7350.
Whitmore, A., 2006. The emperors new clothes: sustainable mining? J. Clean. Prod. 14, 309–314. https://doi.org/10.1016/j.jclepro.2004.10.005.
Xu, J., Fan, L., Xie, Y., Wu, G., 2019. Recycling-equilibrium strategy for phosphogypsum pollution control in phosphate fertilizer plants. J. Clean. Prod. 215, 175–197. https://doi.org/10.1016/j.jclepro.2018.12.236.
Ye, Y., Al-Khaledi, N., Barker, L., Darwish, M.S., El Naggar, A.M.A., El-Yahyaoui, A., Hussein, A., Hussein, E.-S., Shang, D., Taha, M., Zheng, Y., Zhong, J., Haneklaus, N., 2019. Uranium resources in China's phosphate rocks – identifying low-hanging fruits. IOP Conf. Ser. Earth Environ. Sci. 227 https://doi.org/10.1088/1755-1315/227/5/052033.
Zhao, Y., Zang, L., Li, Z., Qin, J., 2012. Discussion on the model of mining circular economy. Energy Procedia 16, 438–443. https://doi.org/10.1016/j.egypro.2012.01.071.
Zhou, Y., Zheng, G., Liu, Z., Liu, R., Tao, C., 2023. Multi-stage precipitation for the eco-friendly treatment of phosphogypsum leachates using hybrid alkaline reagents. J. Water Process Eng. 53, 103626 https://doi.org/10.1016/j.jwpe.2023.103626.